Electronic Supplementary Information

Influence of the electron donor groups on the optical and electrochemical properties of borondifluoride complexes of curcuminoid derivatives: a joint theoretical and experimental study†

Gabriel Canard,*[a] Miguel Ponce-Vargas,[b] Denis Jacquemin,[c,d] Boris Le Guennic,*[b] Abdellah Felouat,[a] Morgane Rivoal,[a] Elena Zaborova,[a] Anthony D'Aléo[a] and Frédéric Fages*[a]

[a] *Aix Marseille Univ, CNRS, CINaM, Campus de Luminy, Case 913, 13288 Marseille, France*

[b] *Institut des Sciences Chimiques de Rennes, UMR 6226 CNRS-Université de Rennes 1, 263 Avenue du Général Leclerc, 35042 Rennes Cedex, France*

[c] *Laboratoire CEISAM, UMR CNRS 6230, Université de Nantes, 2 Rue de la Houssinière, BP 92208, 44322 Nantes Cedex 3, France*

[d] *Institut Universitaire de France, 1 rue Descartes, 75231 Paris Cedex 05, France*

Figure S4. Cyclic voltammograms of nonsymmetrical compounds **16 - 23** (except **17**: see reference 1, and **18**: see publication text) in DCM containing 0.1M of *n*-Bu_4NPF_6 (scan rate: 100 mV/s).

Figure S5. Cyclic voltammograms of compounds **24 - 32** (except **31**: see publication text) in DCM containing *n*-Bu_4NPF_6 (scan rate: 100 mV/s).

Figure S6. Cyclic voltammograms of compounds **2**, **14**, and **32** in DMF containing *n*-Bu_4NPF_6 (scan rate: 100 mV/s).

Figure S7. Plot of the correlation of the reduction potential with Hammett constants.

Figure S8. Reduction potential as a function of the resonance parameters σ^+.

Figure S9. Electronic absorption and fluorescence emission spectra in DCM at room temperature of compounds a/ **1**; b/ **2**; c/ **3**; d/ **4**; e/ **5**; f/ **6**; g/ **7**; h/ **8**; i/ **9**; j/ **10**; k/ **11**; l/ **12**; m/ **13**; n/ **14**; o/ **15**; p/ **16**; q/ **17**; r/ **18**; s/ **19**; t/ **20**; u/ **21**; v/ **22**; w/ **23**; x/ **24**; y/ **25**; z/ **26**; aa/ **27**; ab/ **28**; ac/ **29**; ad/ **30**; ae/ **31** and af/ **32**.

Table S1. Calculated HOMO-LUMO energies and energy gap values for selected molecules (in eV)

	5	**6**	**9**	**10**	**15**	**20**	**23**	**26**	**29**
LUMO	-3,1	-2.9	-2.9	-3.1	-3.2	-3.1	-3.3	-2.9	-3.1
HOMO	-6.1	-6.1	-6.1	-6.3	-5.8	-6.0	-6.4	-6.1	-6.2
Energy gap	3.0	3.2	3.2	3.2	2.6	2.9	3.1	3.2	3.1

Table S2. Theoretical vertical absorption data obtained for selected dyes in DCM solution with TD-DFT.

		Calculated				
		λ_{max}		f	Assignment (%)	
		(nm)	(cm^{-1})			
5	I	521	19194	1.048	HOMO→LUMO	(98.35)
	II	402	24876	0.895	HOMO-2→LUMO	(98.82)
	III	344	29070	0.067	HOMO-3→LUMO	(77.08)
	IV	275	36364	0.049	HOMO-2→LUMO+1	(94.47)
	V	320	31250	0.044	HOMO-1→LUMO+1	(92.81)
6	I	476	21008	2.148	HOMO→LUMO	(99.01)
	II	273	36630	0.185	HOMO-1→LUMO+1	(87.63)
	III	388	25773	0.058	HOMO-1→LUMO	(98.18)
	IV	296	33784	0.055	HOMO→LUMO+1	(95.15)
	V	302	33113	0.046	HOMO-4→LUMO	(90.60)
9	I	471	21231	2.186	HOMO→LUMO	(99.06)
	II	269	37175	0.196	HOMO-1→LUMO+1	(90.05)
	III	257	38911	0.074	HOMO→LUMO +2	(69.71)
	IV	380	26312	0.060	HOMO-1→LUMO	(98.05)
	V	294	34014	0.046	HOMO→LUMO+1	(94.73)
10	I	472	21186	1.733	HOMO→LUMO	(97.63)
	II	360	27778	0.192	HOMO-2→LUMO	(97.49)
	III	282	35461	0.092	HOMO-1→LUMO+1	(83.55)
	IV	335	29851	0.067	HOMO-3→LUMO	(88.65)
	V	249	40161	0.053	HOMO-3→LUMO+1	(60.94)
15	I	612	16 340	1.032	HOMO→LUMO	(98.05)
	II	346	28 902	0.566	HOMO-4→LUMO	(91.00)
	III	391	25 575	0.104	HOMO-1→LUMO+1	(78.29)
	IV	359	27 855	0.065	HOMO-3→LUMO	(88.55)
	V	534	18 727	0.027	HOMO-1→LUMO	(99.27)
20	I	539	18553	1.495	HOMO→LUMO	(97.70)
	II	430	23256	0.635	HOMO-1→LUMO	(94.66)
	III	356	28090	0.258	HOMO→LUMO+1	(94.07)
	IV	328	30488	0.236	HOMO-3→LUMO	(61.93)
	V	309	32362	0.041	HOMO-1→LUMO+1	(67.27)
23	I	472	21186	1.872	HOMO→LUMO	(98.10)
	II	361	27701	0.415	HOMO-1→LUMO	(92.02)
	III	266	37594	0.178	HOMO-1→LUMO+1	(89.95)
	IV	313	31949	0.090	HOMO→LUMO+1	(87.97)
	V	302	33113	0.026	HOMO-3→LUMO	(82.16)
26	I	479	20877	2.106	HOMO→LUMO	(99.10)
	II	273	36630	0.278	HOMO-1→LUMO+1	(92.53)
	III	387	25840	0.019	HOMO-1→LUMO	(98.01)
	IV	322	31056	0.016	HOMO-4→LUMO	(99.01)
	V	312	32051	0.007	HOMO-3→LUMO	(94.03)
29	I	480	20833	2.099	HOMO→LUMO	(99.08)
	II	389	25707	0.017	HOMO-1→LUMO	(98.15)
	III	308	32468	0.017	HOMO-5→LUMO	(71.54)
					HOMO-4→LUMO	(24.71)
	IV	312	32051	0.009	HOMO-2→LUMO	(95.65)
	V	305	32787	0.006	HOMO-4→LUMO	(68.15)

Table S3: Half-wave potential (*vs*. Fc/Fc^+) of compounds **2**, **14**, **32** in DMF

Dye	$E_{1/2}^{red}$ (V)	$E_{1/2}^{ox}$ (V)	ΔE (V)[c]
2	-0.91	-	-
14	-1.53[a]	0.24	1.71
32	-1.32 -0.78	-	-

[a] Pseudo-reversible redox process

Multi Linear Regression (MLR) fit of the electrochemical data.

The regression model can be written as: $Y = B_0 + B_1X_1 + ... + B_kX_k + e$

Table S4. Regression coefficients of the models ($X_1 = \sum\sigma_{term}$, $X_2 = \sum\sigma_{meso}$).

	Predicted Y	Parameter	Value	Error	t-Value	Prob> |t|
Eq. 3	$E_{1/2}^{red1}$	B_0	-1.15683	0.01136	-101.83048	<0.0001
		B_1	0.16223	0.01308	12.40689	<0.0001
		B_2	0.05043	0.05223	0.96548	0.37159
Eq. 4	$E_{1/2}^{red1}$	B_0	-1.06623	0.0124	-85.99894	<0.0001
		B_1	0.10214	0.00676	15.1192	<0.0001
		B_2	0.0444	0.0247	1.79751	0.13218

B_x: regression coefficients

Table S5. Statistics of linear regression between predicted and measured values for the MLR models.

Predicted Y	R^2 [a]	Adj. R-Square[b]	RMSE –(SD)[c]
Eq. 3	0.96248	0.94998	0.02864
Eq. 4	0.97894	0.97051	0.02297

[a] R^2: Correlation coefficient; [b] SEC: Determination coefficient; [c] Root Mean Square Error – Standard Deviation

Table S6. Regression coefficients of the models (X_1= ΔE (eV), Eq. 5).

Predicted Y	Parameter	Value	Error	t-Value	Prob> |t|
E_{em} (eV)	B_0	0.52041	0.19718	2.63921	0.0141
	B_1	0.72022	0.09101	7.91366	<0.0001

B_x: regression coefficients

Table S7. Maximum absorption wavelengths and molar absorption coefficients for the lowest-energy absorption band and fluorescence emission quantum yields of compounds **1** - **32** in DCM.

Compound	λ_{abs} **(nm)**	E_{abs} **(eV)**	ε **/ M^{-1}cm^{-1}**	ϕ_f
1	421	2.95	58700	0.19
2	426	2.91	43980	0.18
3	433	2.86	41000	0.08
4	503	2.47	86200	0.55
5	496	2.50	68700	0.13
6	503	2.47	71500	0.45
7	464	2.67	55600	0.145
8	498	2.49	76750	0.345
9	488	2.54	75480	0.44
10	476	2.61	65900	0.32

11	502	2.47	80450	0.50
12	524	2.37	84 860	0.52
13	597	2.08	48400	0.425
14	619	2.00	59900	0.39
15	554	2.24	69400	0.05
16	559	2.22	51400	0.12
17	511	2.43	74 510	0.46
18	583	2.13	54350	0.005
19	601	2.06	52100	0.01
20	536	2.31	59800	0.55
21	517	2.40	55900	0.04
22	495	2.51	77500	0.46
23	471	2.63	48600	0.32
24	506	2.45	74100	0.39
25	506	2.45	73200	0.41
26	505	2.46	78230	0.41
27	508	2.44	60000	0.42
28	507	2.45	72100	0.41
29	507	2.45	74770	0.42
30	519	2.39	87500	0.52
31	615	2.02	68900	0.40
32	439	2.82	55750	0.06

Figure S1. ^{1}H and ^{13}C NMR spectra.

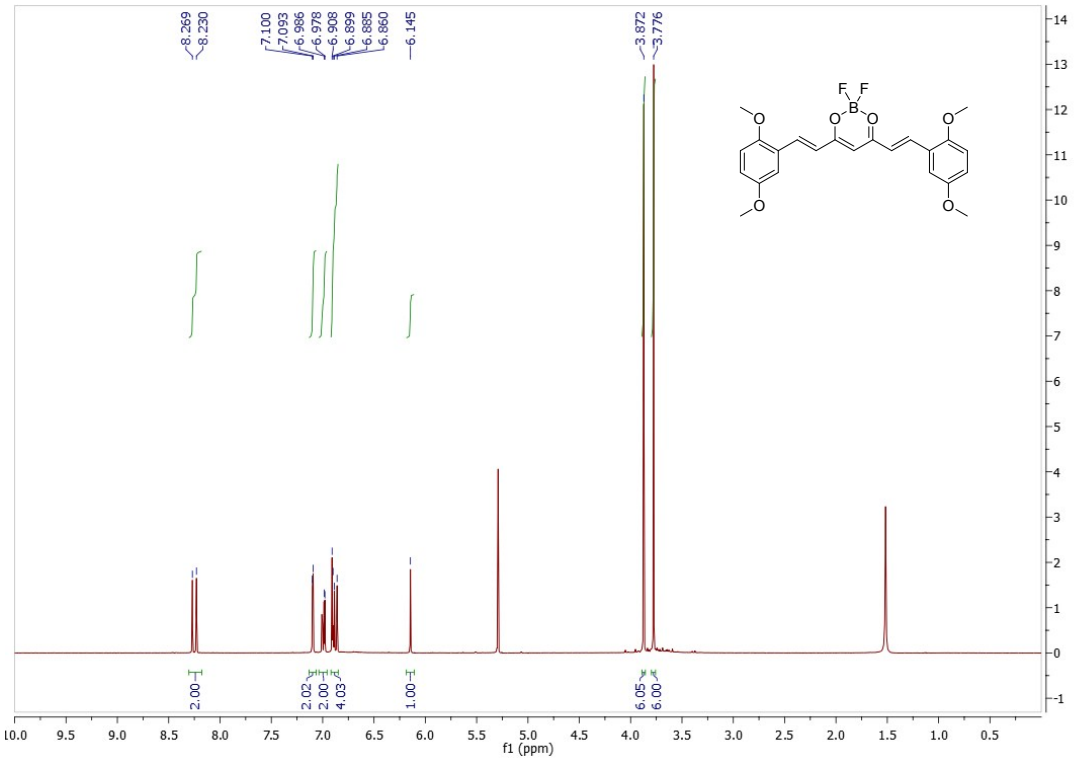

Figure NMR1. ^{1}H NMR spectrum of **5** (4,6-bis((E)-2,5-dimethoxystyryl)-2,2-difluoro-2H-1,3,2-dioxaborinin-1-ium-2-uide)

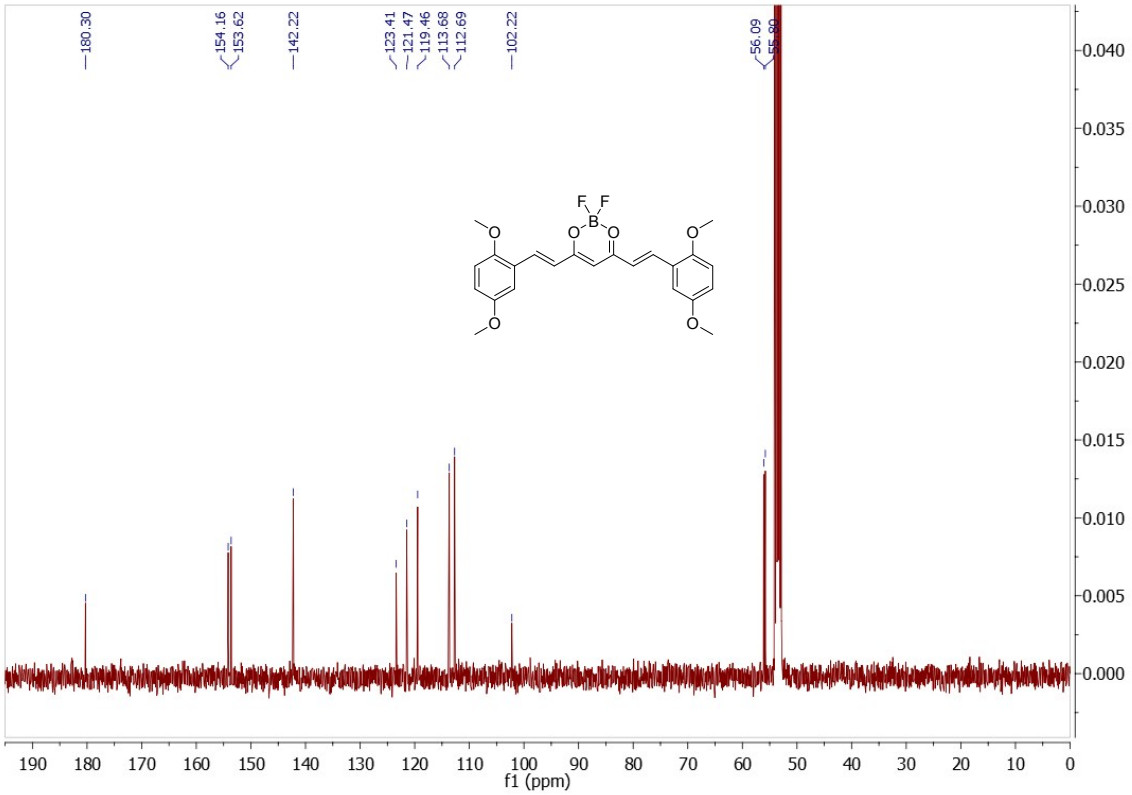

Figure NMR2. ^{13}C NMR spectrum of **5** (4,6-bis((E)-2,5-dimethoxystyryl)-2,2-difluoro-2H-1,3,2-dioxaborinin-1-ium-2-uide)

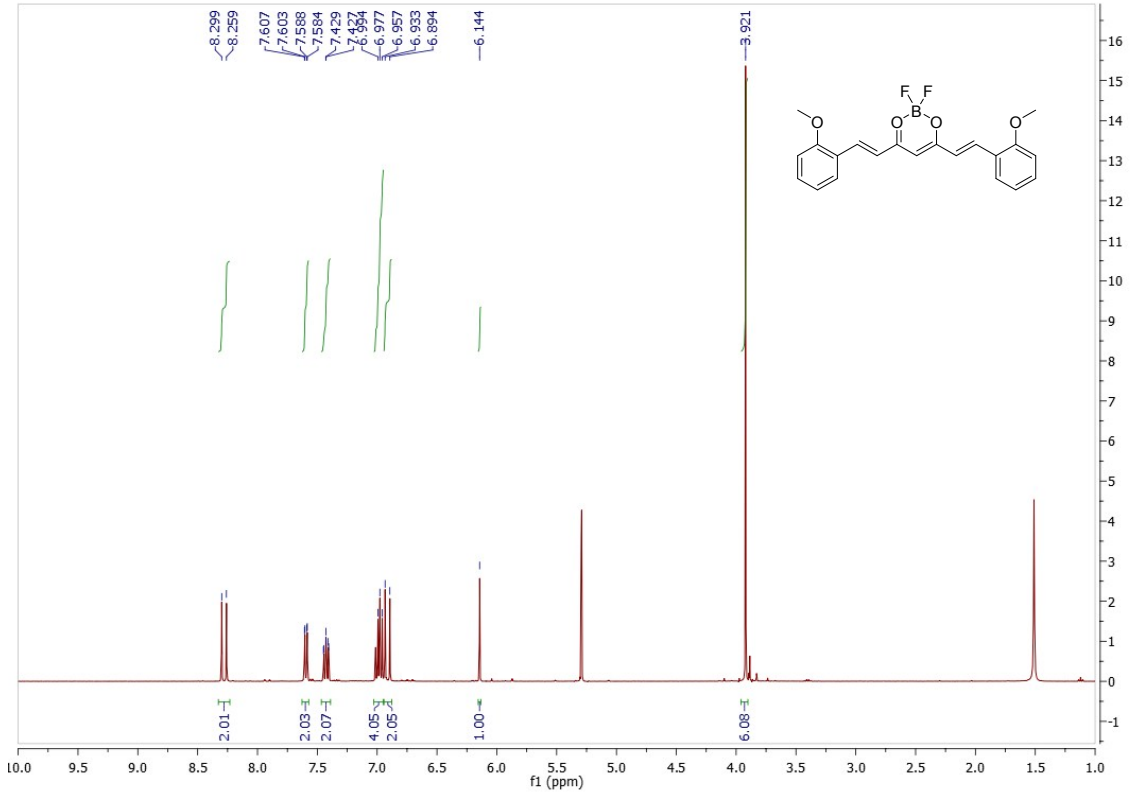

Figure NMR3. ^{1}H NMR spectrum of **10** (2,2-difluoro-4,6-bis((E)-2-methoxystyryl)-2H-1,3,2-dioxaborinin-1-ium-2-uide)

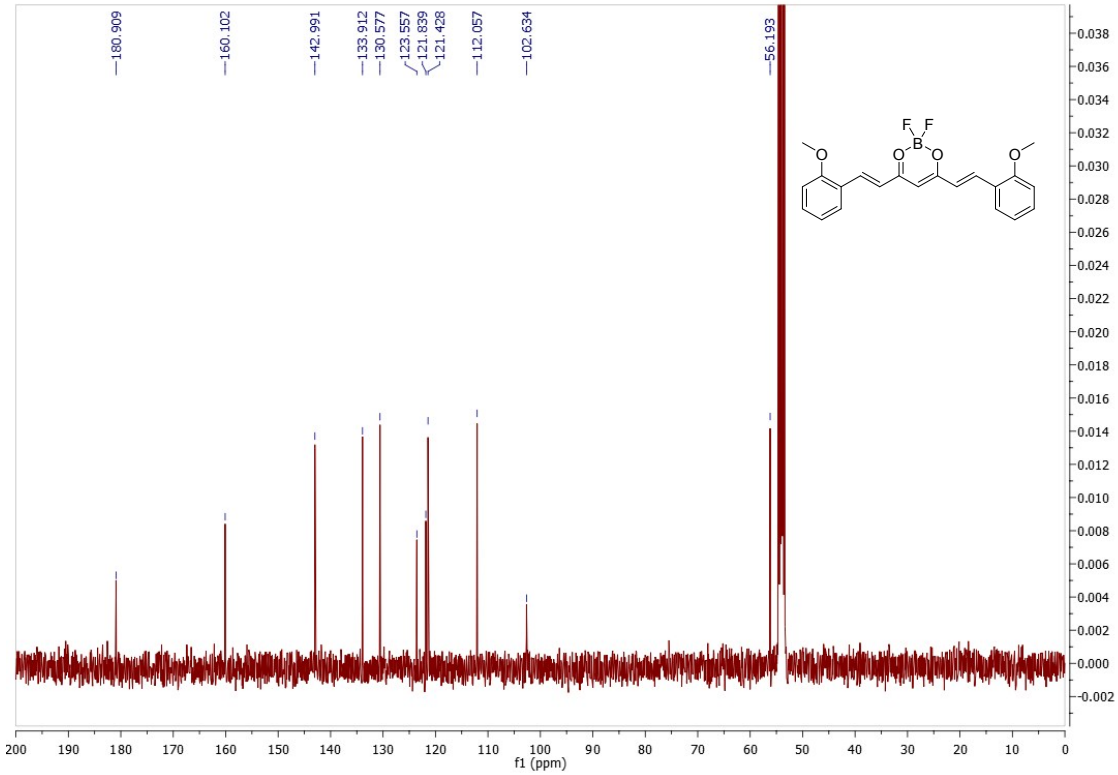

Figure NMR4. ^{13}C NMR spectrum of **10** (2,2-difluoro-4,6-bis((E)-2-methoxystyryl)-2H-1,3,2-dioxaborinin-1-ium-2-uide)

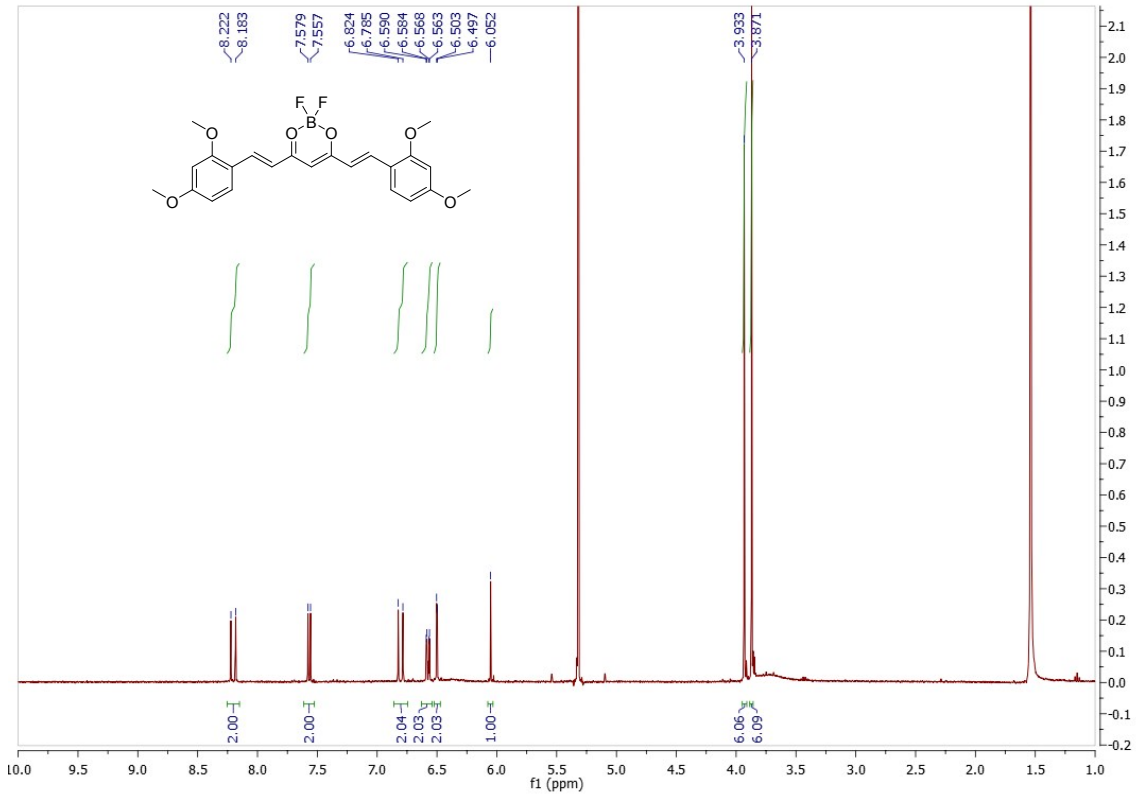

Figure NMR5. ^{1}H NMR spectrum of **11** (4,6-bis((E)-2,4-dimethoxystyryl)-2,2-difluoro-2H-1,3,2-dioxaborinin-1-ium-2-uide)

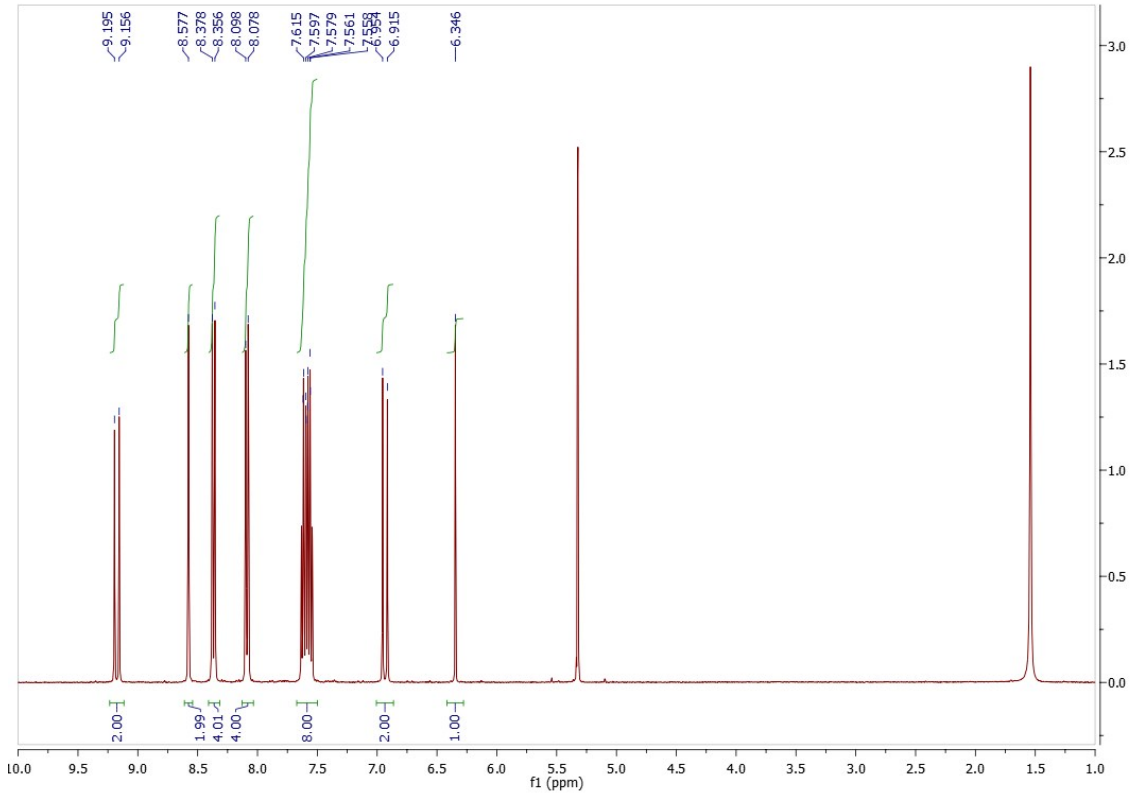

Figure NMR6. ^{1}H NMR spectrum of **15** (4,6-bis((E)-2-(anthracen-9-yl)vinyl)-2,2-difluoro-2H-1,3,2-dioxaborinin-1-ium-2-uide)

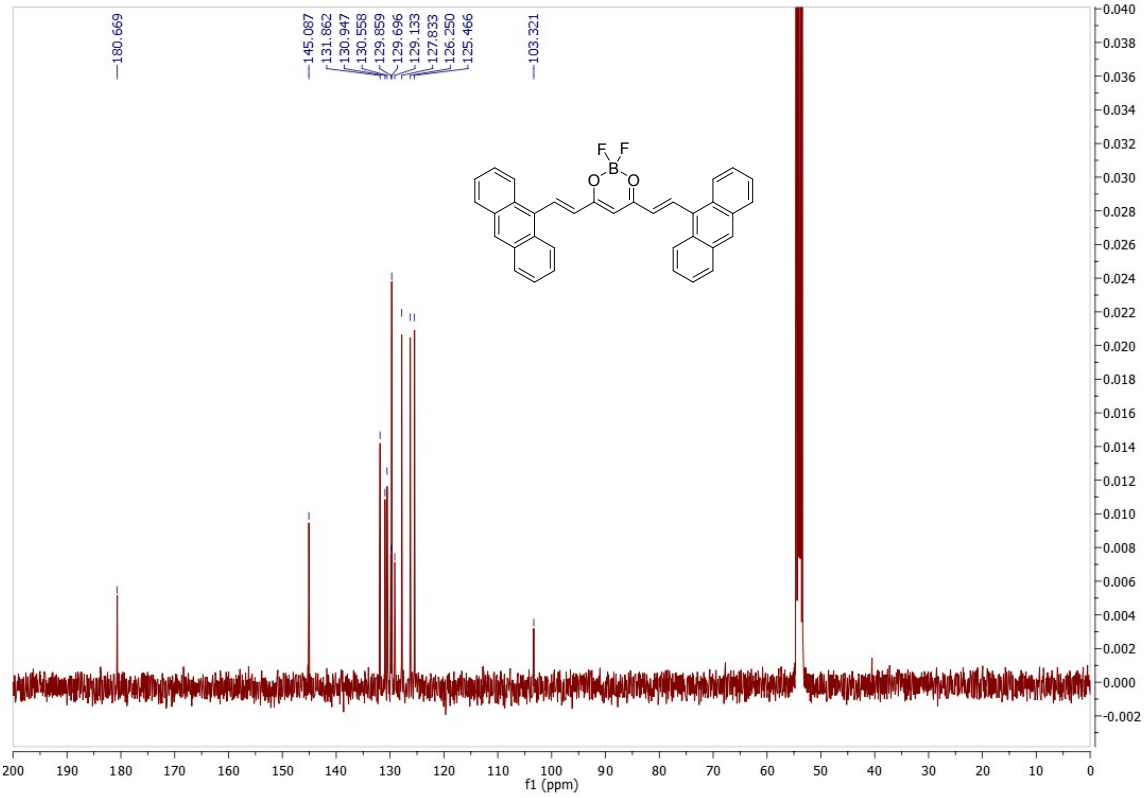

Figure NMR7. ^{13}C NMR spectrum of **15** (4,6-bis((E)-2-(anthracen-9-yl)vinyl)-2,2-difluoro-2H-1,3,2-dioxaborinin-1-ium-2-uide)

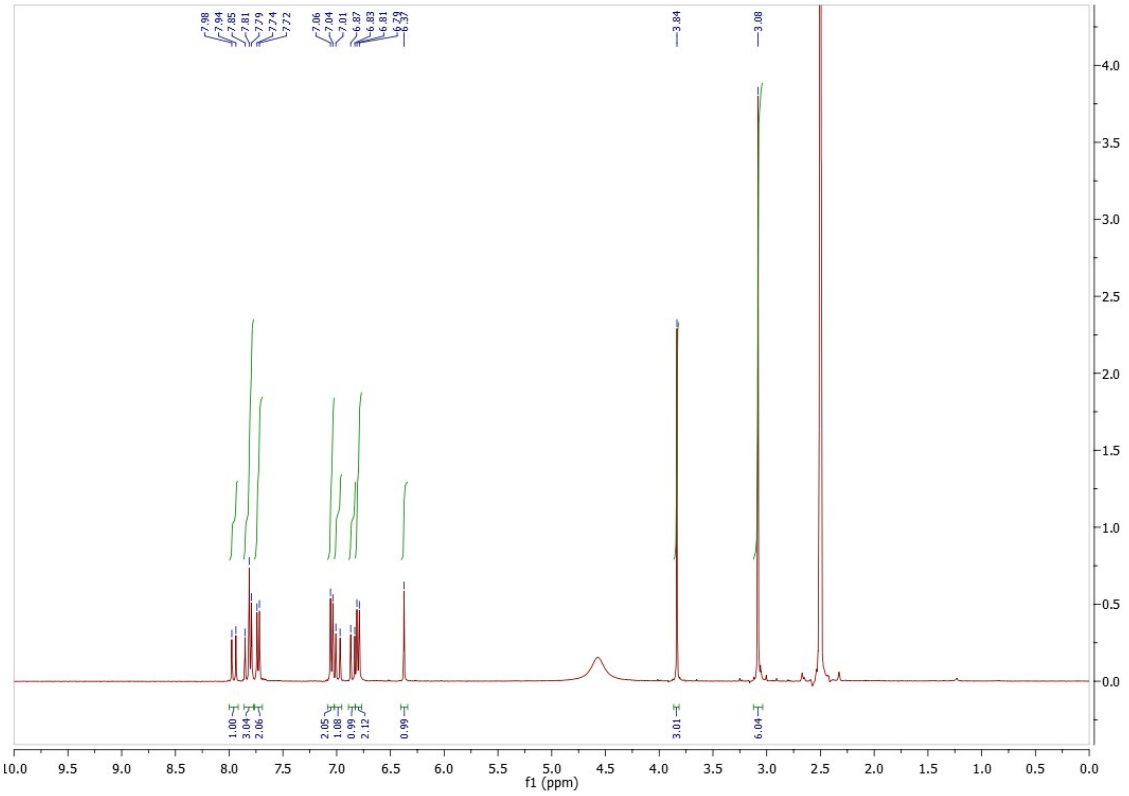

Figure NMR8. ^{1}H NMR spectrum of **16** (6-((E)-4-(dimethylamino)styryl)-2,2-difluoro-4-((E)-4-methoxystyryl)-2H-1,3,2-dioxaborinin-1-ium-2-uide)

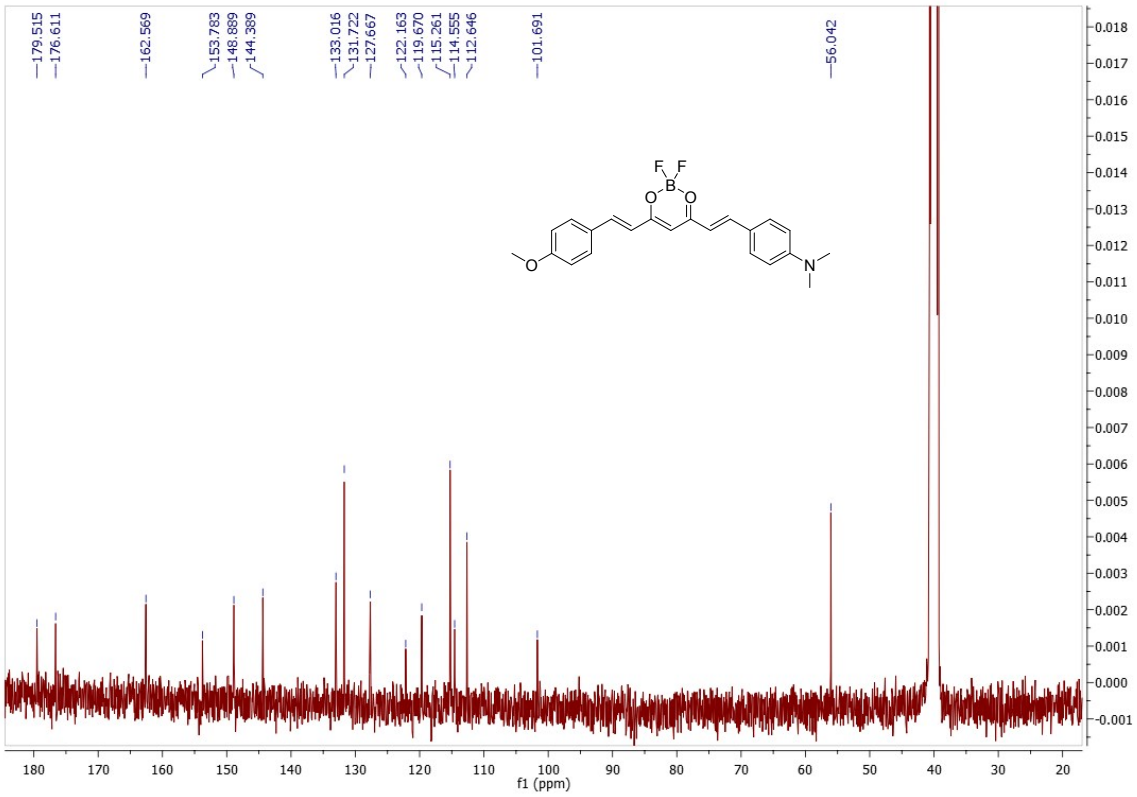

Figure NMR9. ^{13}C NMR spectrum of **16** (6-((E)-4-(dimethylamino)styryl)-2,2-difluoro-4-((E)-4-methoxystyryl)-2H-1,3,2-dioxaborinin-1-ium-2-uide)

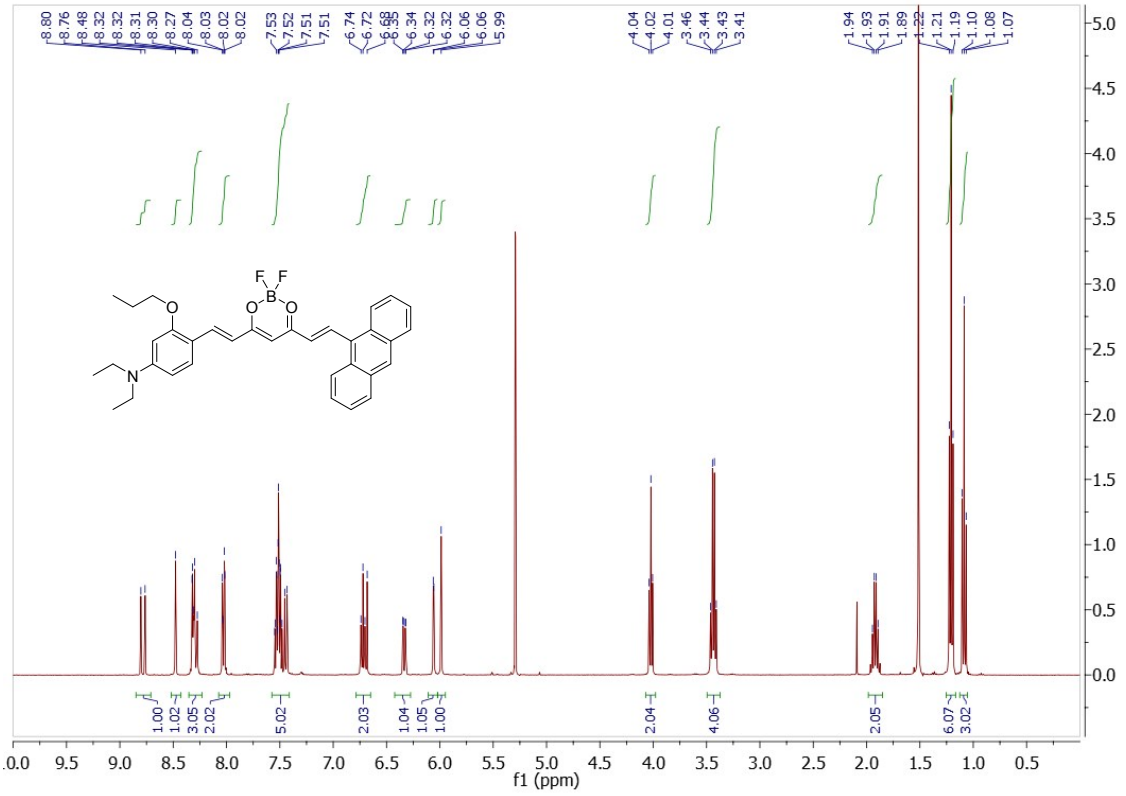

Figure NMR10. ^{1}H NMR spectrum of **18** (4-((E)-2-(anthracen-9-yl)vinyl)-6-((E)-4-(diethylamino)-2-propoxystyryl)-2,2-difluoro-2H-1,3,2-dioxaborinin-1-ium-2-uide)

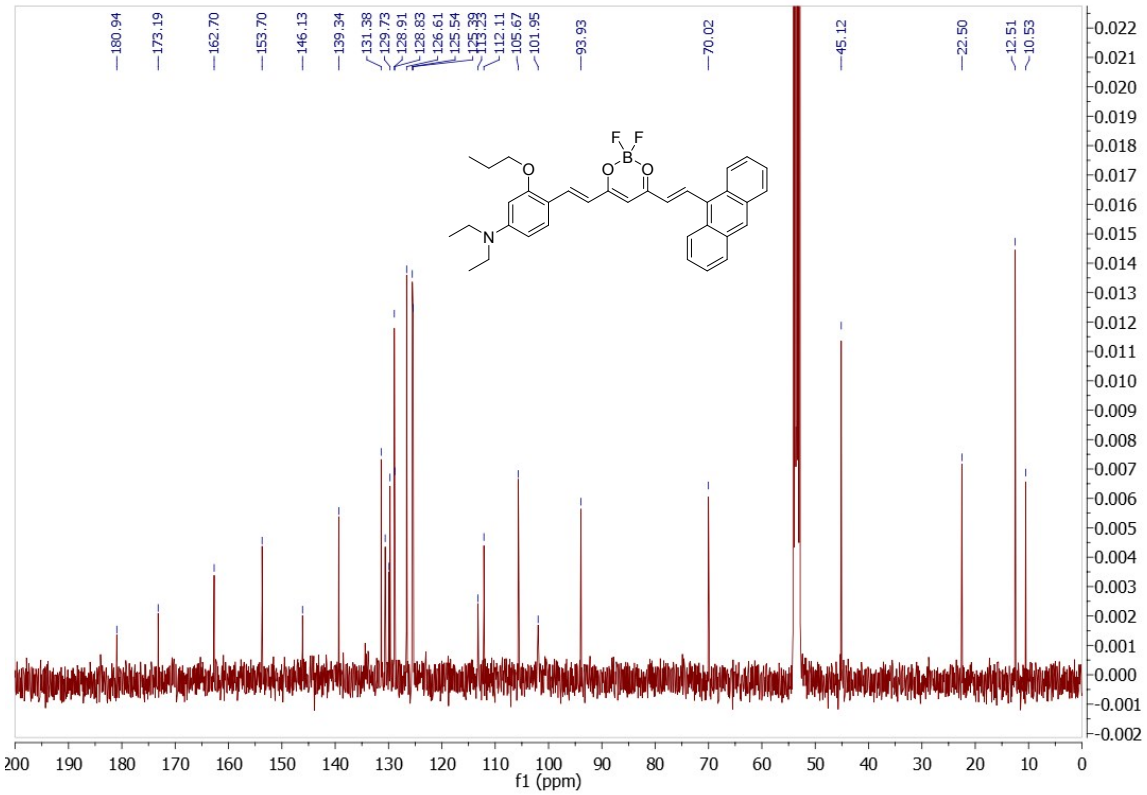

Figure NMR11. ^{13}C NMR spectrum of **18** (4-((E)-2-(anthracen-9-yl)vinyl)-6-((E)-4-(diethylamino)-2-propoxystyryl)-2,2-difluoro-2H-1,3,2-dioxaborinin-1-ium-2-uide)

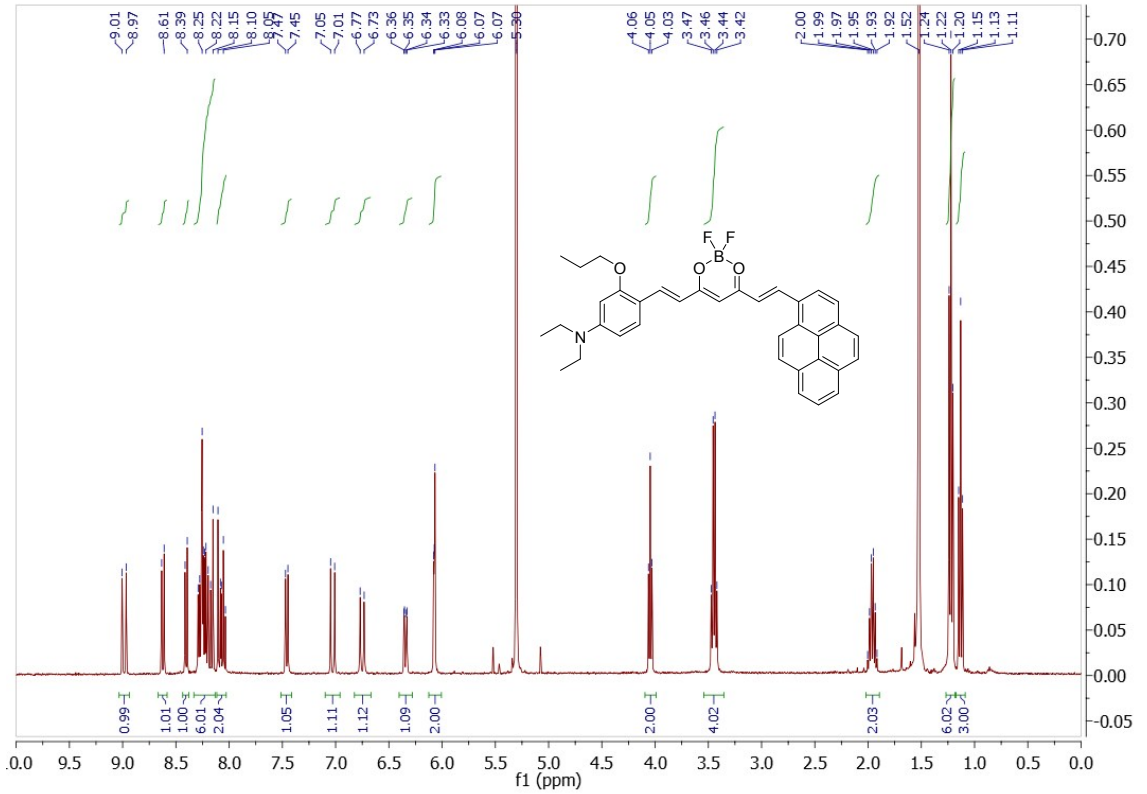

Figure NMR12. ^{1}H NMR spectrum of **19** (6-((E)-4-(diethylamino)-2-propoxystyryl)-2,2-difluoro-4-((E)-2-(pyren-1-yl)vinyl)-2H-1,3,2-dioxaborinin-1-ium-2-uide)

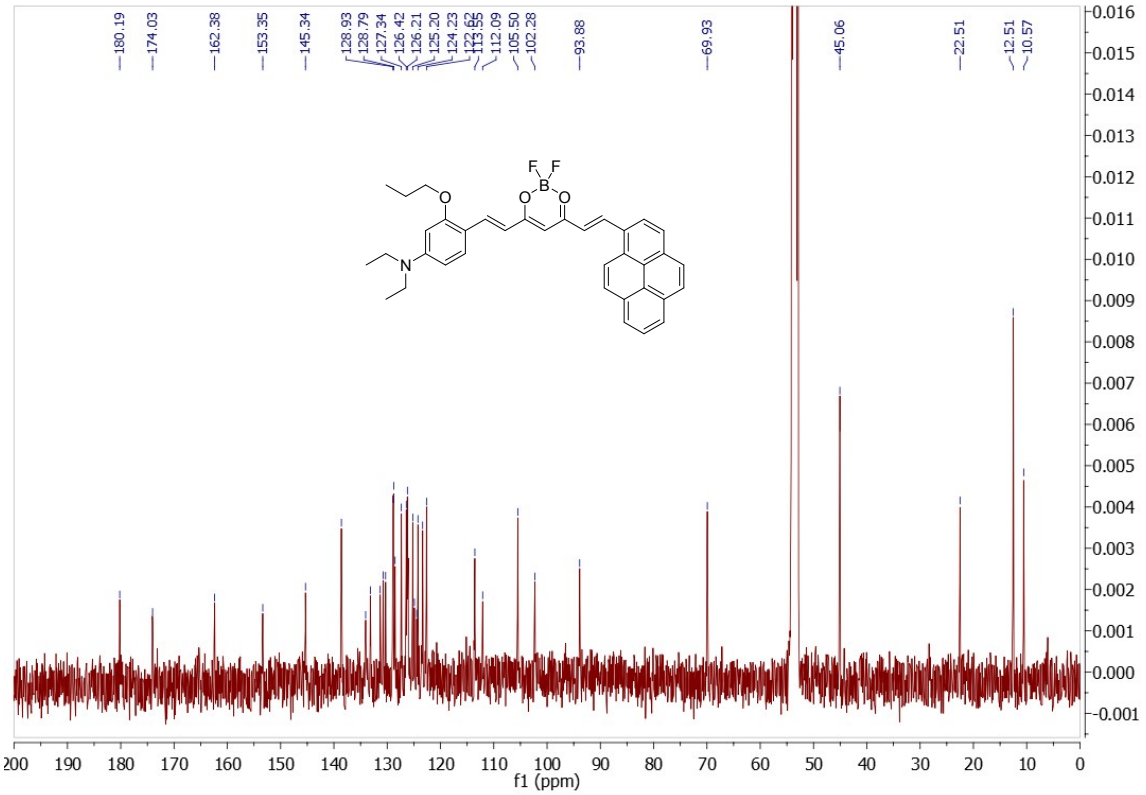

Figure NMR13. ^{13}C NMR spectrum of **19** (6-((E)-4-(diethylamino)-2-propoxystyryl)-2,2-difluoro-4-((E)-2-(pyren-1-yl)vinyl)-2H-1,3,2-dioxaborinin-1-ium-2-uide)

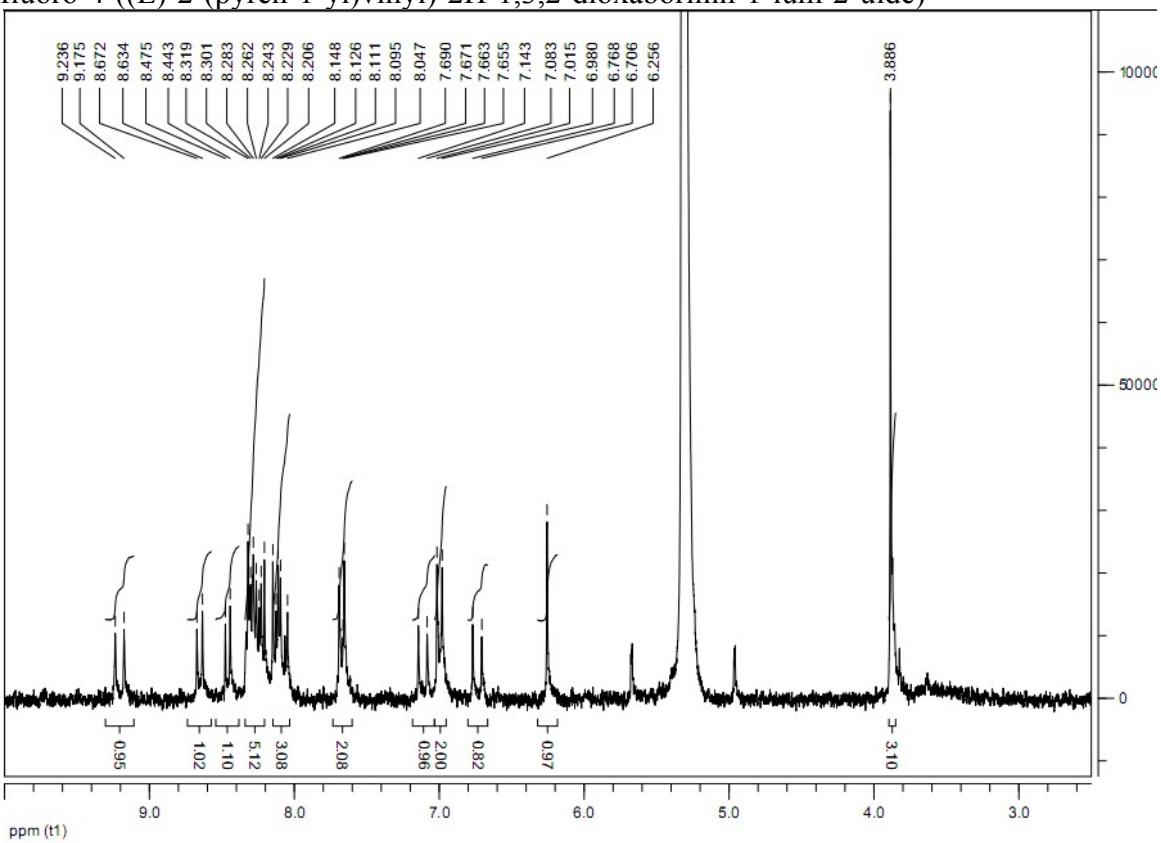

Figure NMR14. ^{1}H NMR spectrum of **20** (2,2-difluoro-6-((E)-4-methoxystyryl)-4-((E)-2-(pyren-1-yl)vinyl)-2H-1,3,2-dioxaborinin-1-ium-2-uide)

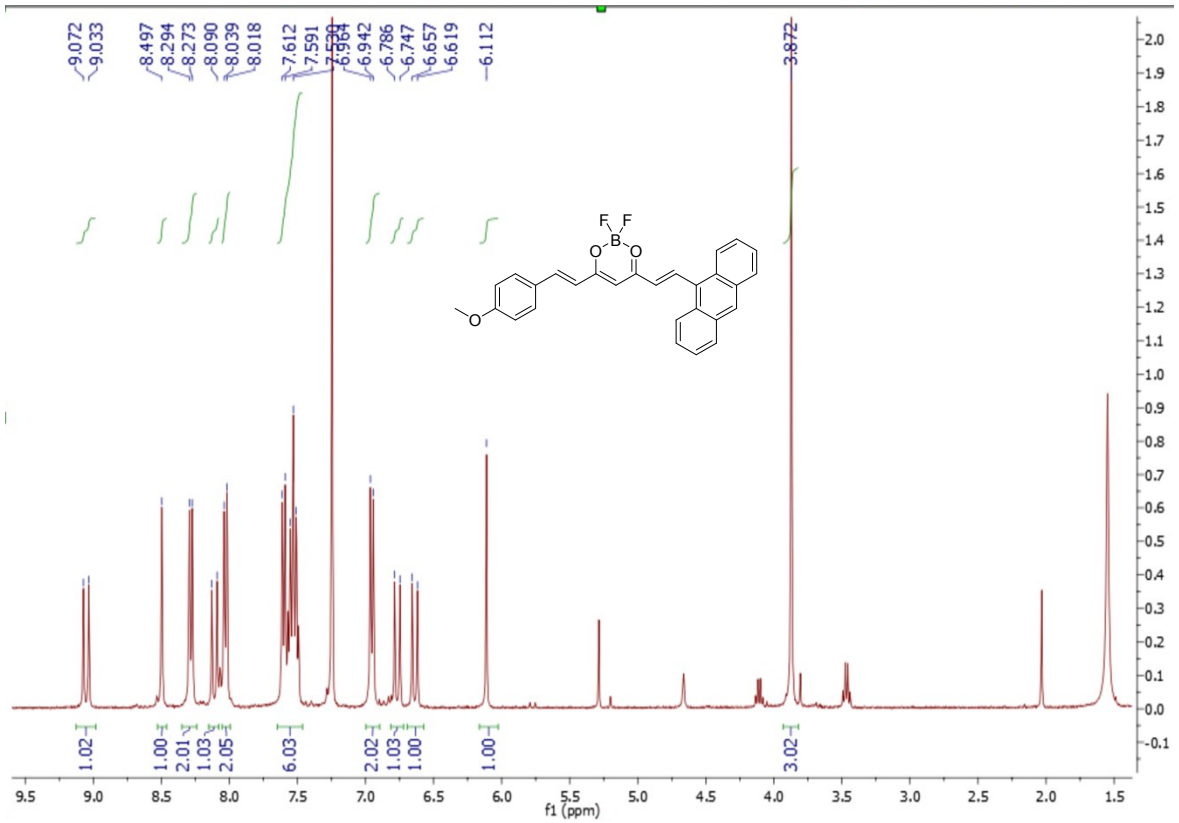

Figure NMR15. ^{1}H NMR spectrum of **21** (4-((E)-2-(anthracen-9-yl)vinyl)-2,2-difluoro-6-((E)-4-methoxystyryl)-2H-1,3,2-dioxaborinin-1-ium-2-uide)

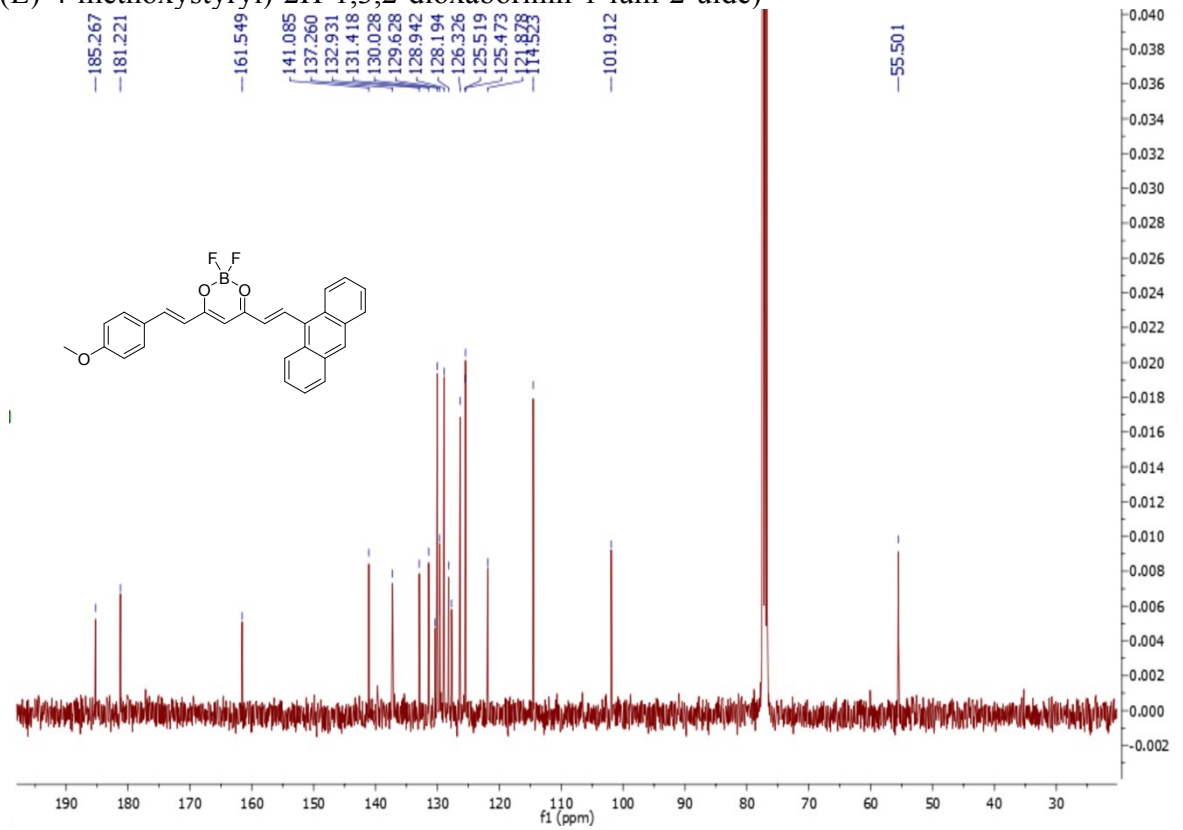

Figure NMR16. ^{13}C NMR spectrum of **21** (4-((E)-2-(anthracen-9-yl)vinyl)-2,2-difluoro-6-((E)-4-methoxystyryl)-2H-1,3,2-dioxaborinin-1-ium-2-uide)

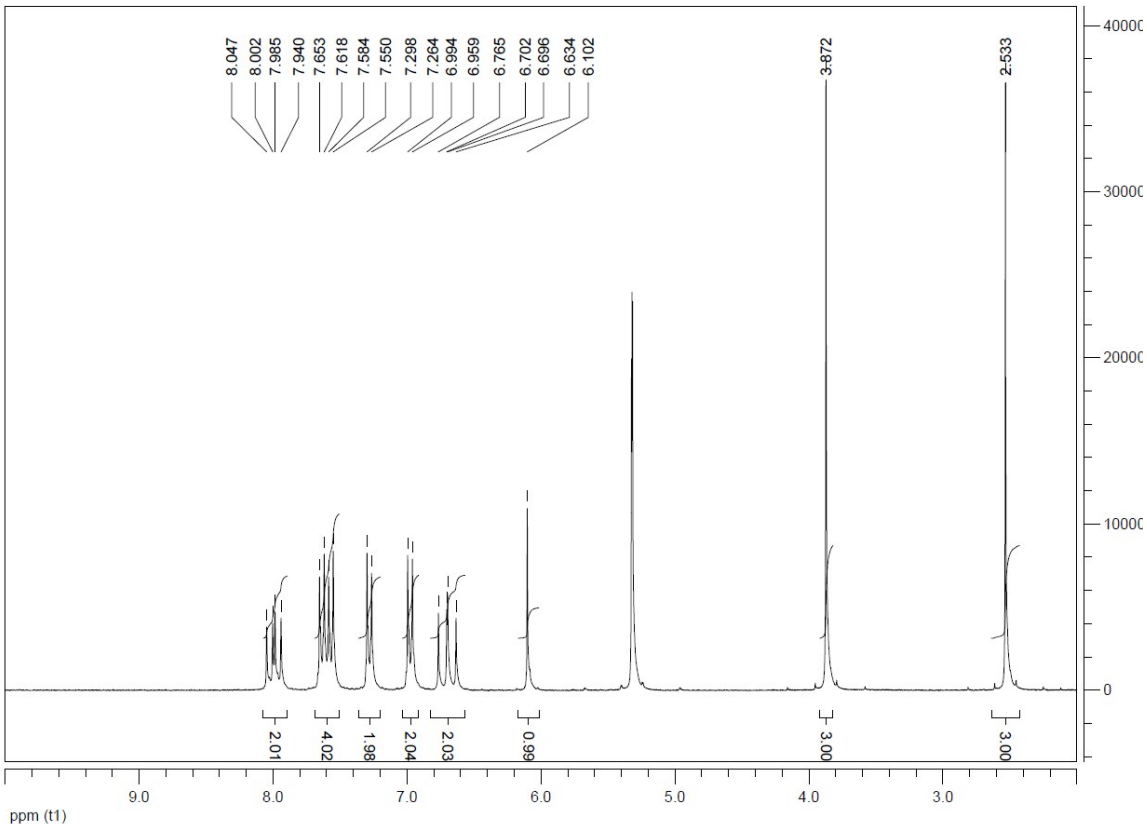

Figure NMR17. ^{1}H NMR spectrum of **22** (2,2-difluoro-6-((E)-4-methoxystyryl)-4-((E)-4-(methylthio)styryl)-2H-1,3,2-dioxaborinin-1-ium-2-uide)

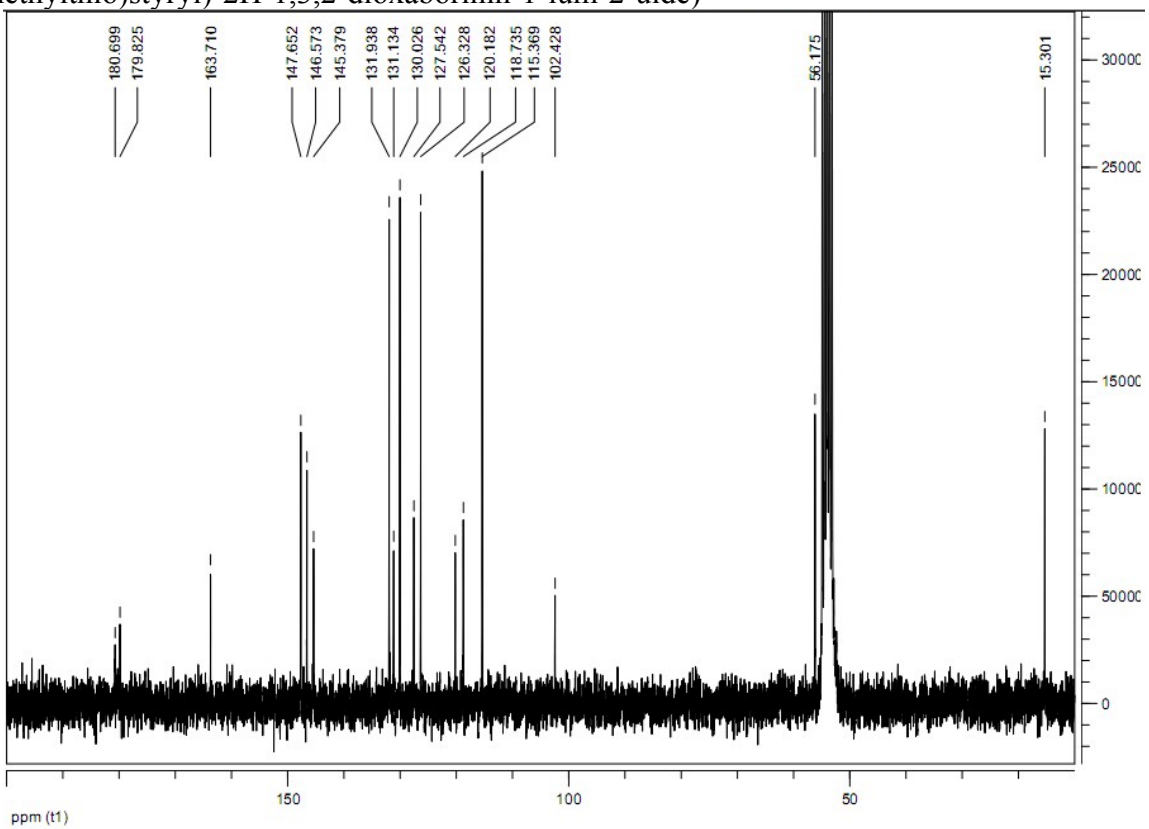

Figure NMR18. ^{13}C NMR spectrum of **22** (2,2-difluoro-6-((E)-4-methoxystyryl)-4-((E)-4-(methylthio)styryl)-2H-1,3,2-dioxaborinin-1-ium-2-uide)

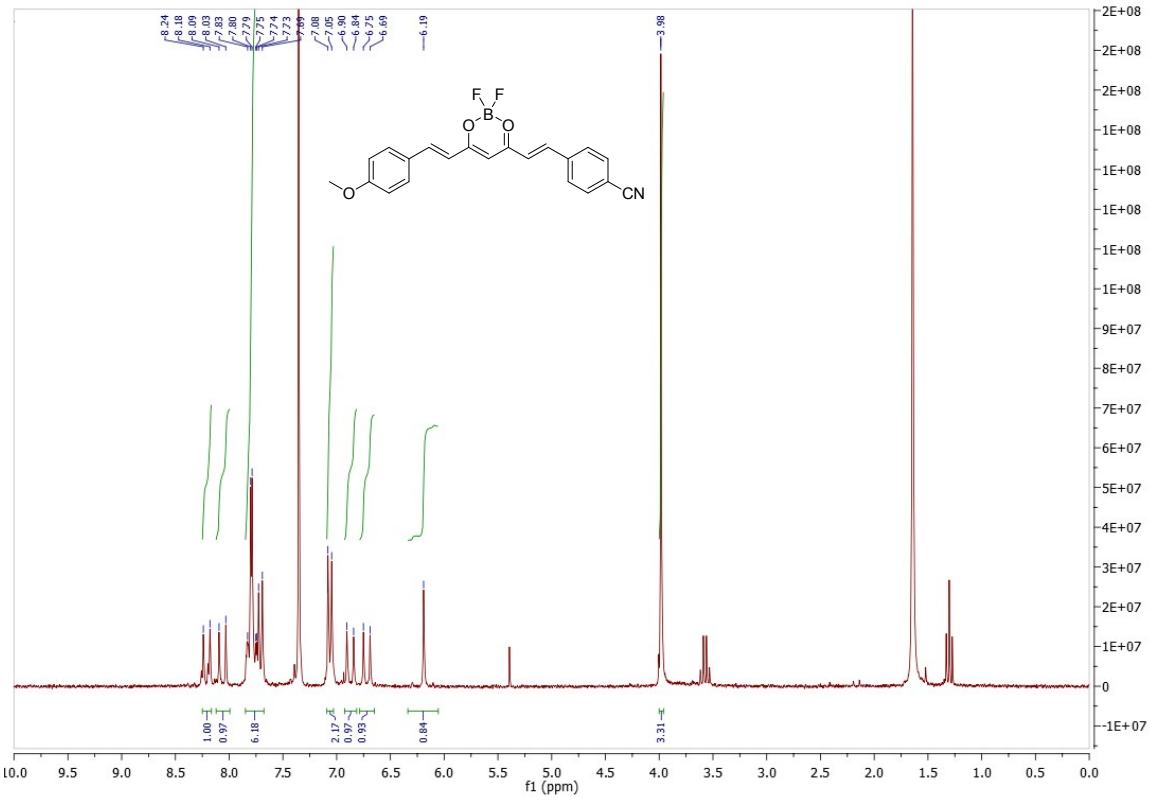

Figure NMR19. ^{1}H NMR spectrum of **23** (4-((E)-4-cyanostyryl)-2,2-difluoro-6-((E)-4-methoxystyryl)-2H-1,3,2-dioxaborinin-1-ium-2-uide)

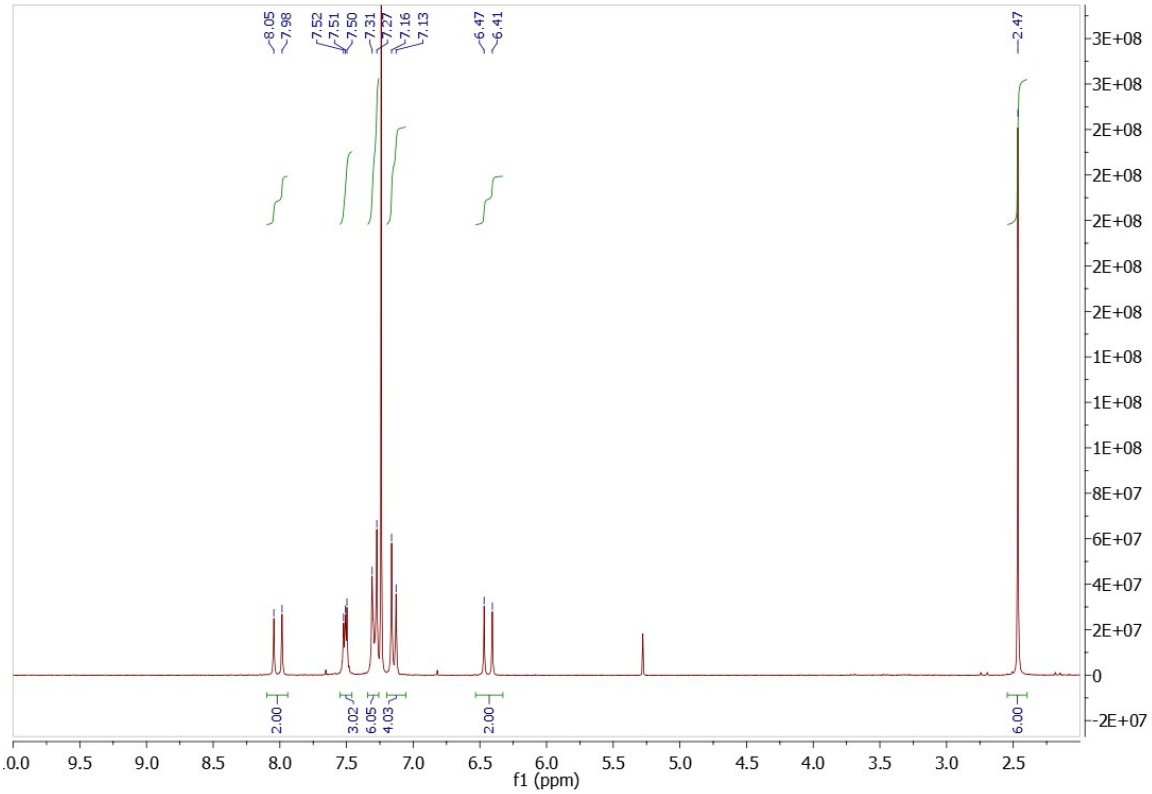

Figure NMR20. ^{1}H NMR spectrum of **30** (2,2-difluoro-4,6-bis((E)-4-(methylthio)styryl)-5-phenyl-2H-1,3,2-dioxaborinin-1-ium-2-uide)

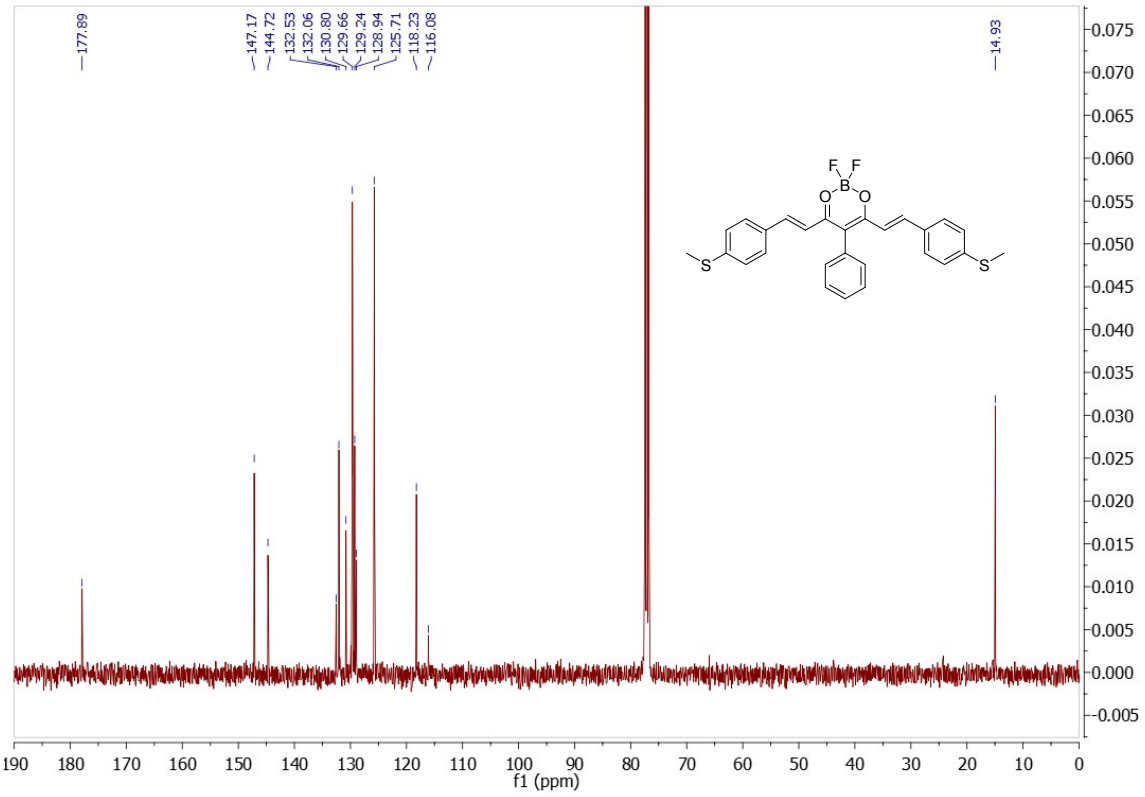

Figure NMR21. ^{13}C NMR spectrum of **30** (2,2-difluoro-4,6-bis((E)-4-(methylthio)styryl)-5-phenyl-2H-1,3,2-dioxaborinin-1-ium-2-uide)

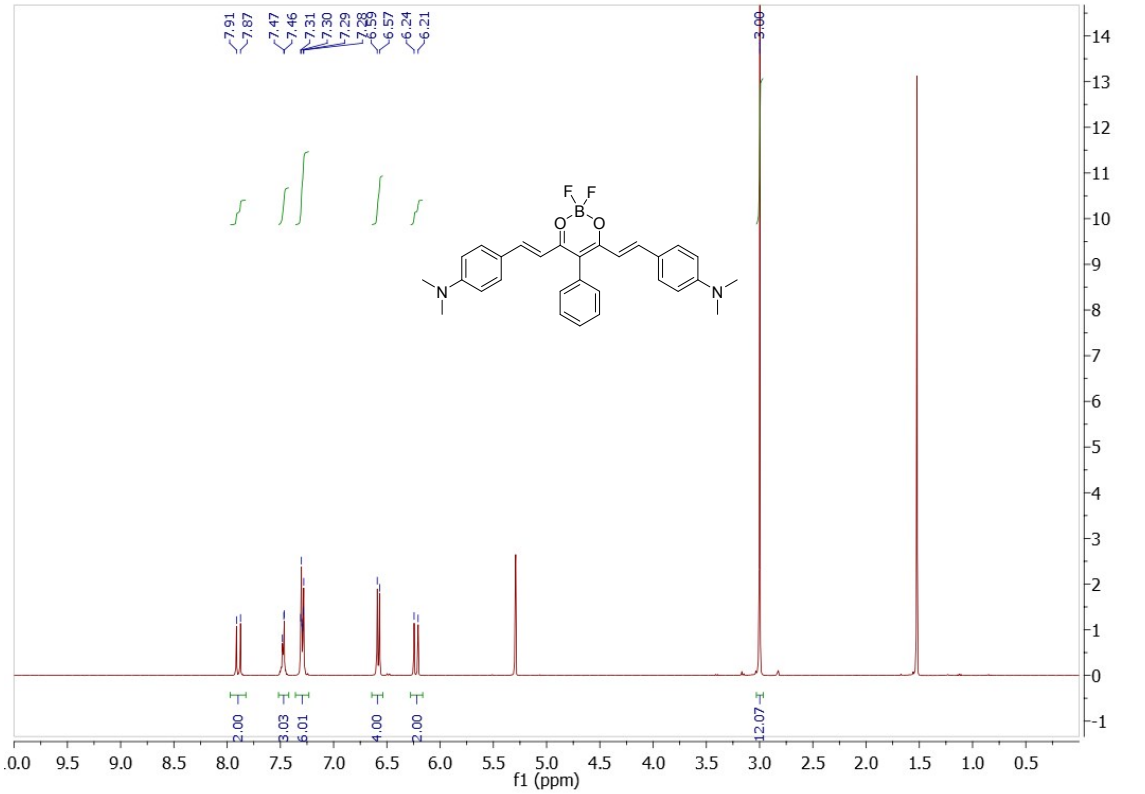

Figure NMR22. ^{1}H NMR spectrum of **31** (4,6-bis((E)-4-(dimethylamino)styryl)-2,2-difluoro-5-phenyl-2H-1,3,2-dioxaborinin-1-ium-2-uide)

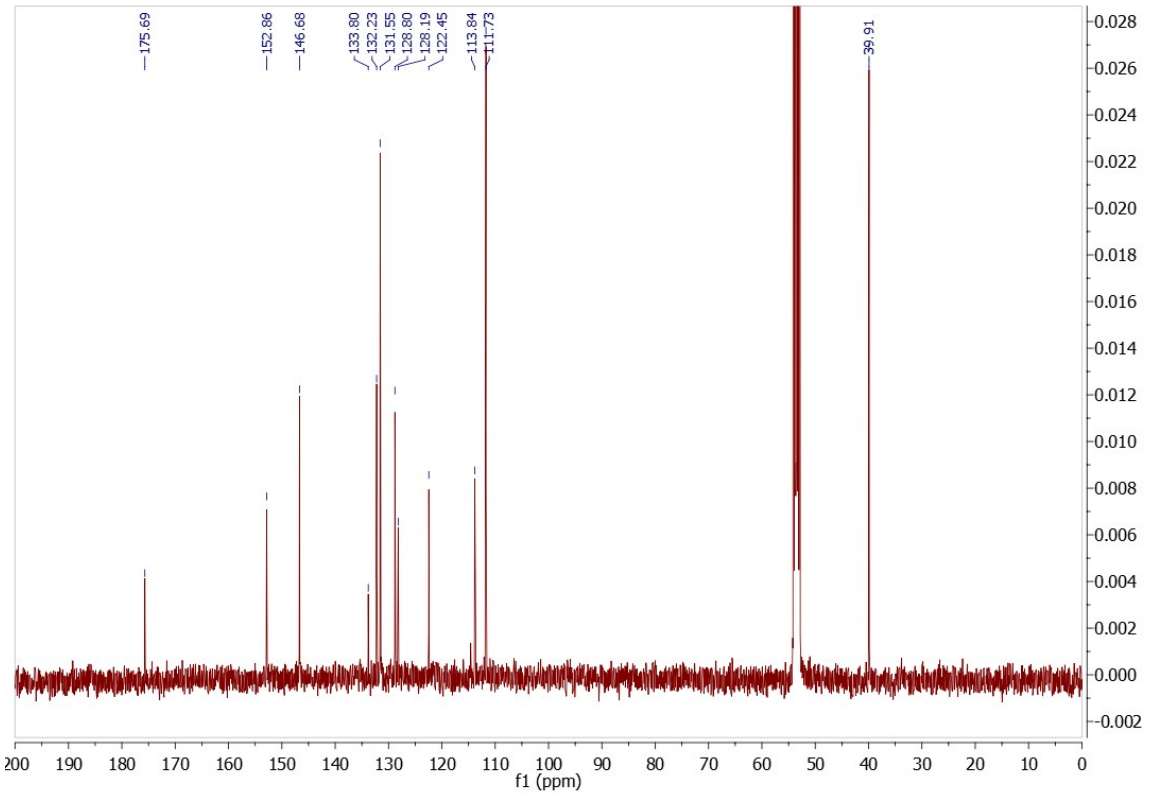

Figure NMR23. ^{13}C NMR spectrum of **31** (4,6-bis((E)-4-(dimethylamino)styryl)-2,2-difluoro-5-phenyl-2H-1,3,2-dioxaborinin-1-ium-2-uide)

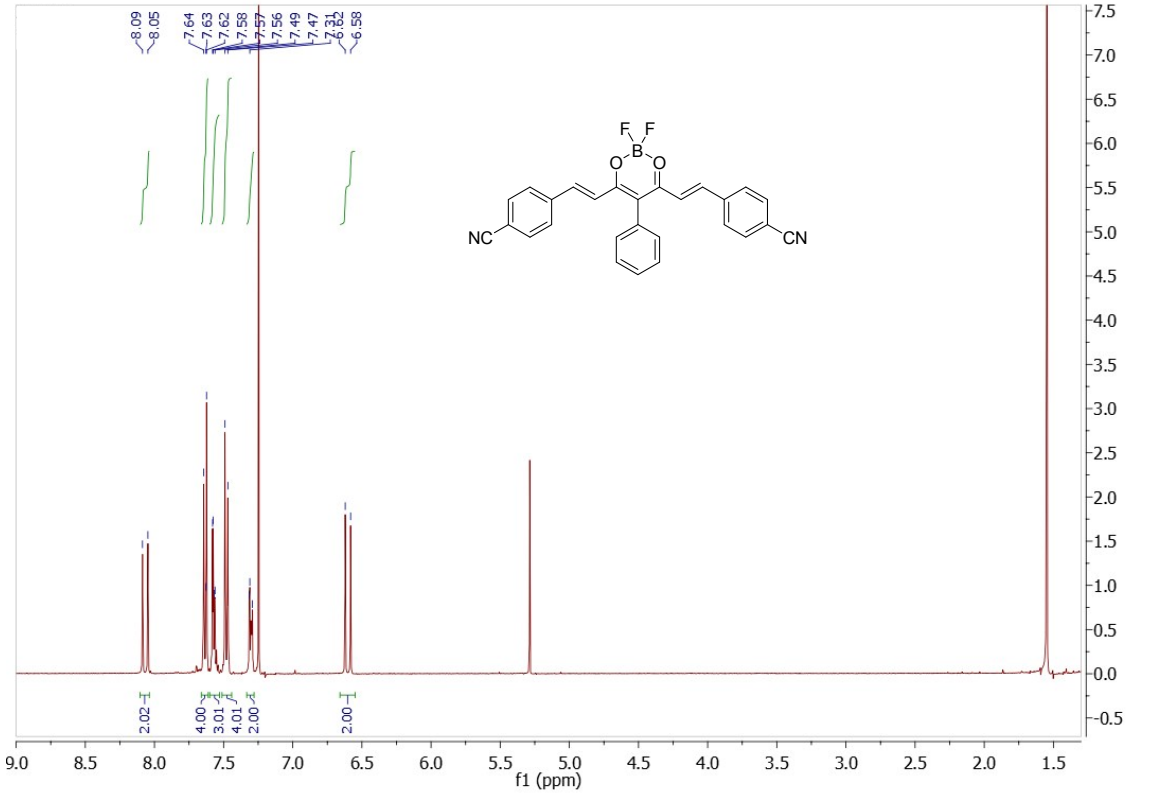

Figure NMR24. ^{1}H NMR spectrum of **32** (4,6-bis((E)-4-cyanostyryl)-2,2-difluoro-5-phenyl-2H-1,3,2-dioxaborinin-1-ium-2-uide)

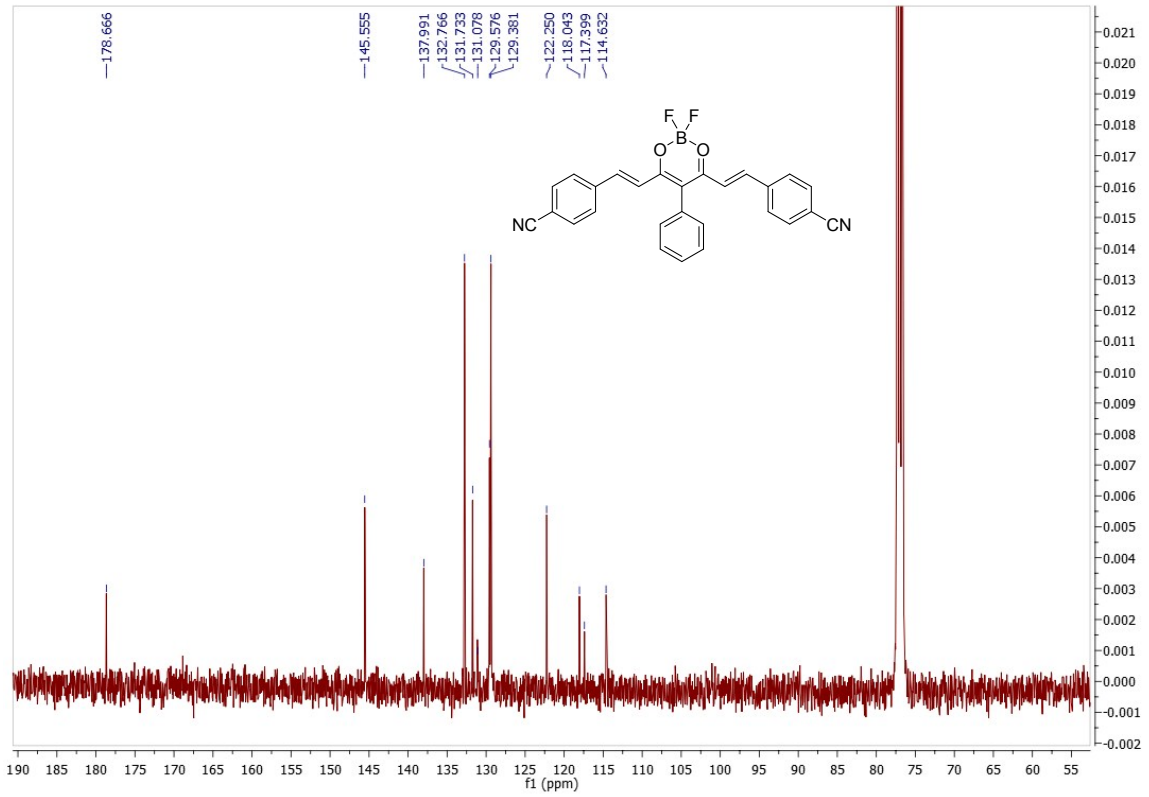

Figure NMR25. ^{13}C NMR spectrum of **32** (4,6-bis((E)-4-cyanostyryl)-2,2-difluoro-5-phenyl-2H-1,3,2-dioxaborinin-1-ium-2-uide)

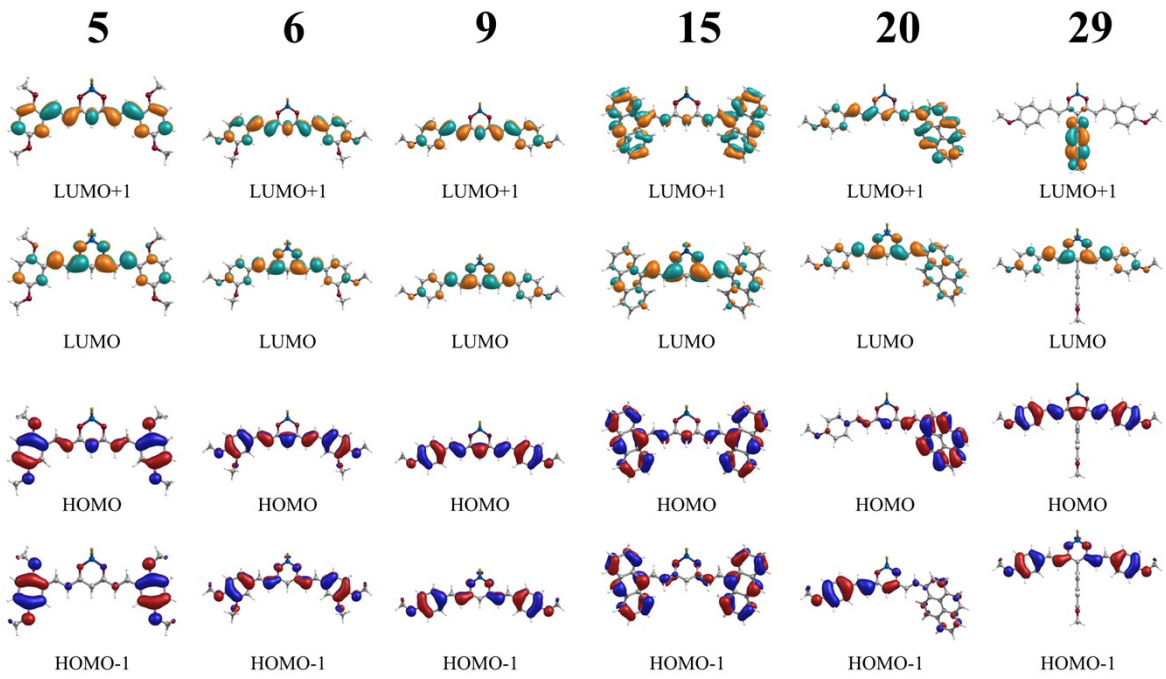

Figure S2. HOMO, HOMO-1, LUMO and LUMO+1 isosurfaces of compounds **5**, **6**, **9**, **15**, **20**, **29**. A contour threshold of 0.03 a.u. has been used.

1

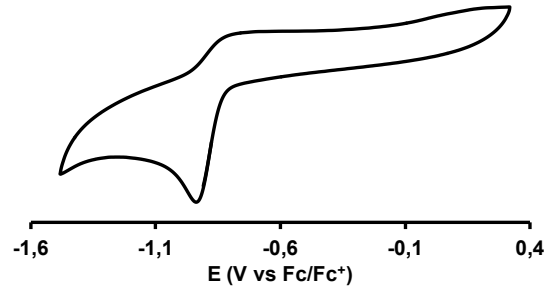
-1,6
-1,1
-0,6
-0,1
0,4
E (V vs Fc/Fc+)

2

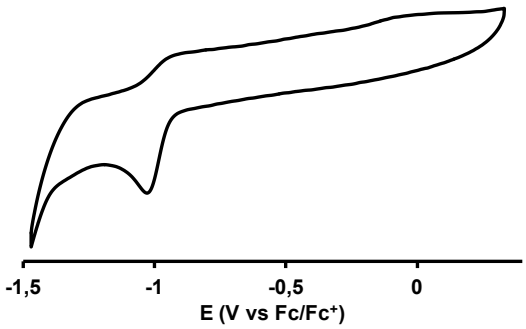
-1,5
-1
-0,5
0
E (V vs Fc/Fc+)

3

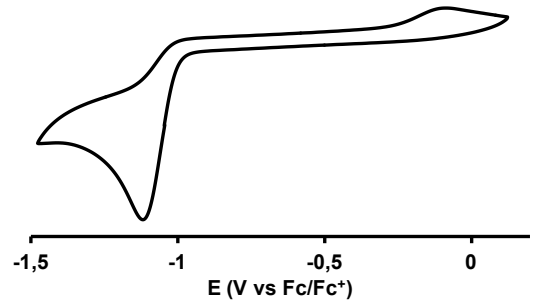
-1,5
-1
-0,5
0
E (V vs Fc/Fc+)

4

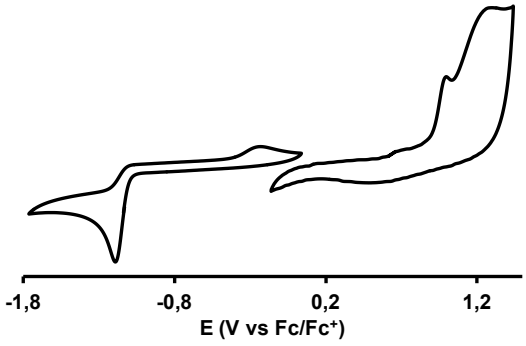
-1,8
-0,8
0,2
1,2
E (V vs Fc/Fc+)

5

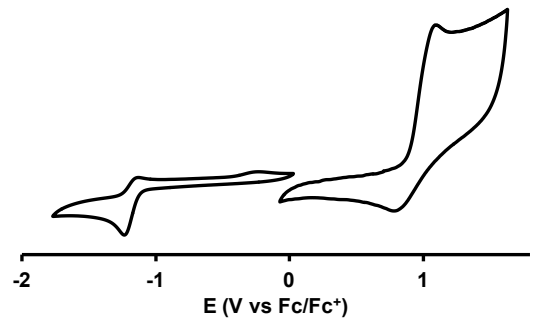
-2
-1
0
1
E (V vs Fc/Fc+)

6

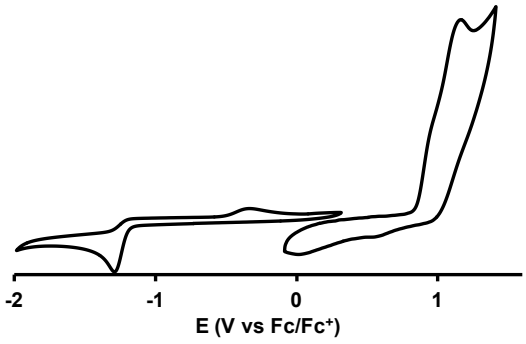
-2
-1
0
1
E (V vs Fc/Fc+)

7

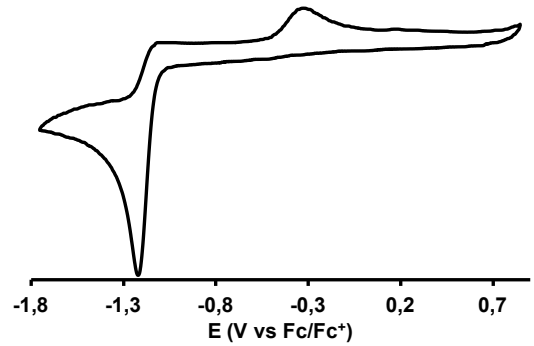
-1,8
-1,3
-0,8
-0,3
0,2
0,7
E (V vs Fc/Fc+)

8

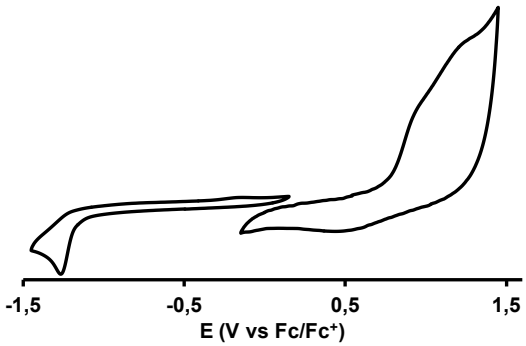
-1,5
-0,5
0,5
1,5
E (V vs Fc/Fc+)

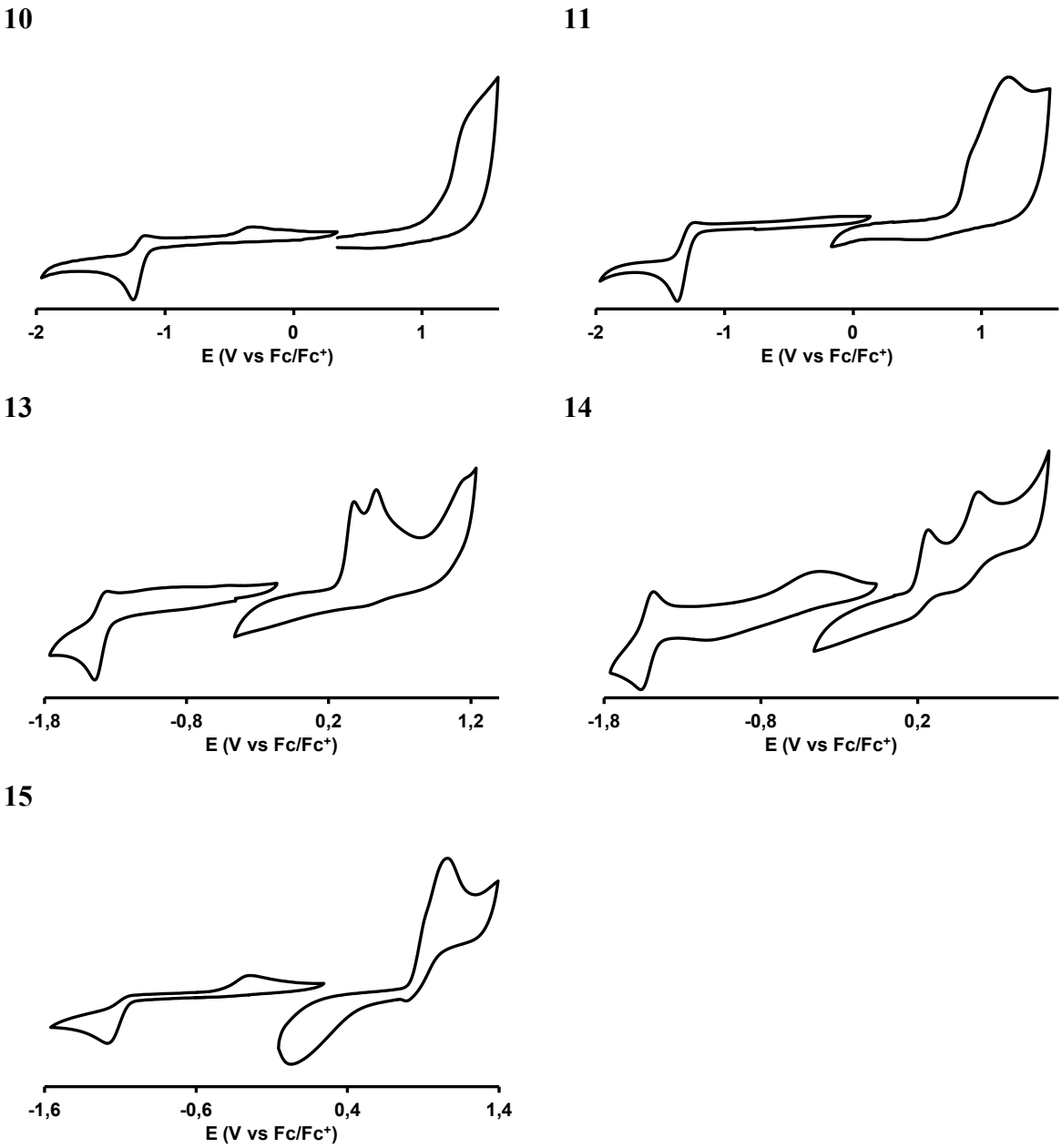

Figure S3. Cyclic voltammograms of symmetrical compounds **1** - **15** in DCM (except compounds **9** and **12**, see reference 1) containing 0.1M of *n*-Bu_4NPF_6 (scan rate: 100 mV/s).

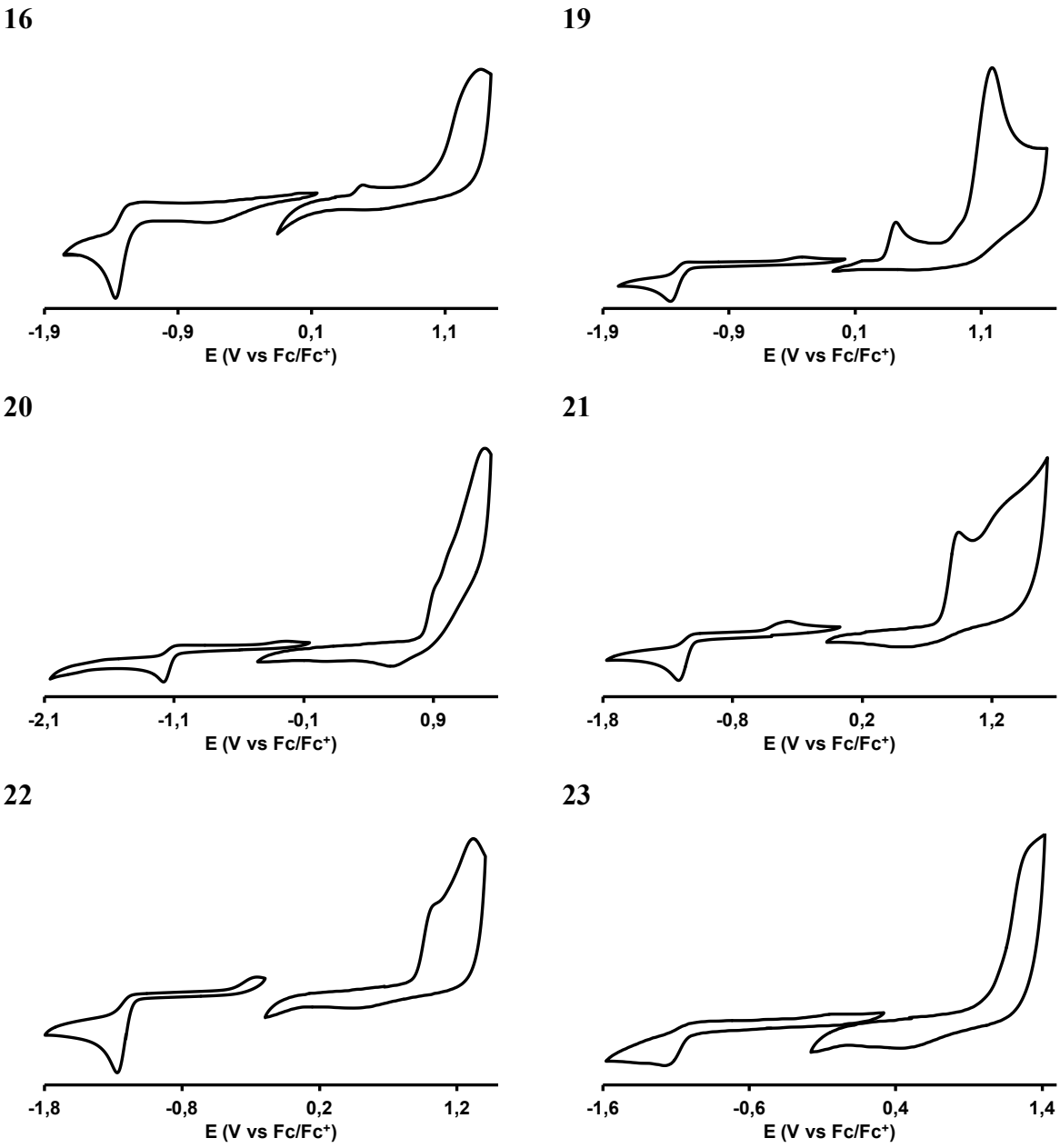

Figure S4. Cyclic voltammograms of nonsymmetrical compounds **16** - **23** (except **17**: see reference 1, and **18**: see text) in DCM containing 0.1M of *n*-Bu_4NPF_6 (scan rate: 100 mV/s).

24

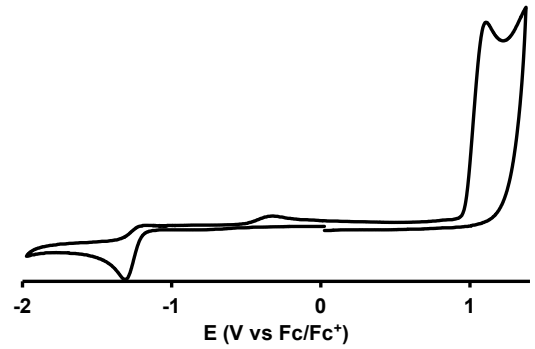

25

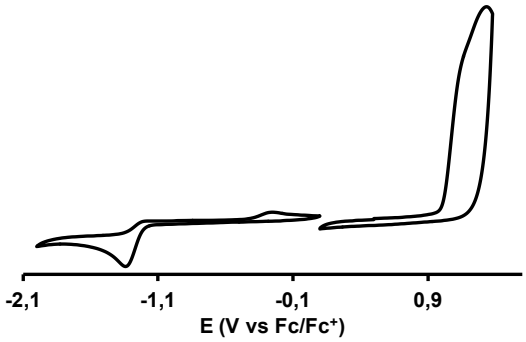

26

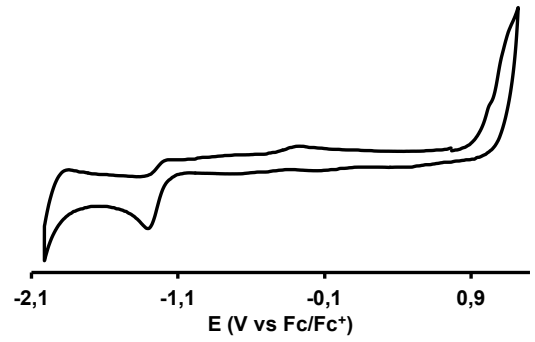

27

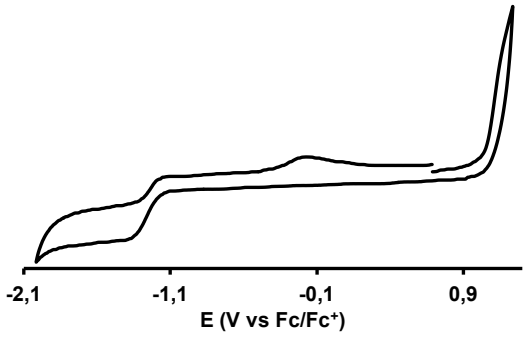

28

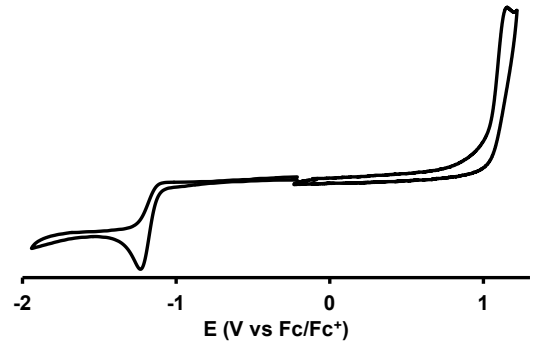

29

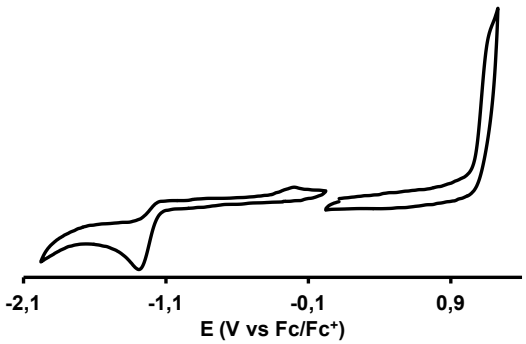

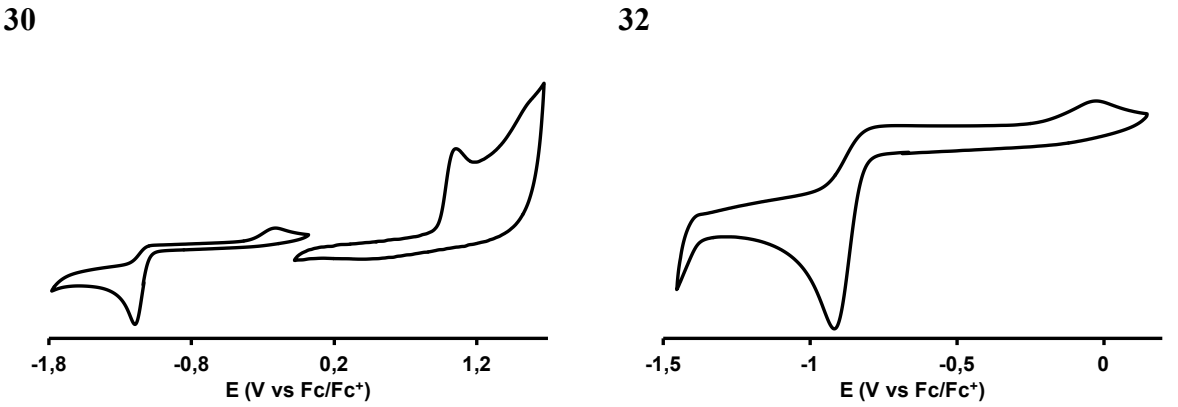

Figure S5. Cyclic voltammograms of compounds **24** - **32** (except **31**: see publication text) in DCM containing *n*-Bu_4NPF_6 (scan rate: 100 mV/s).

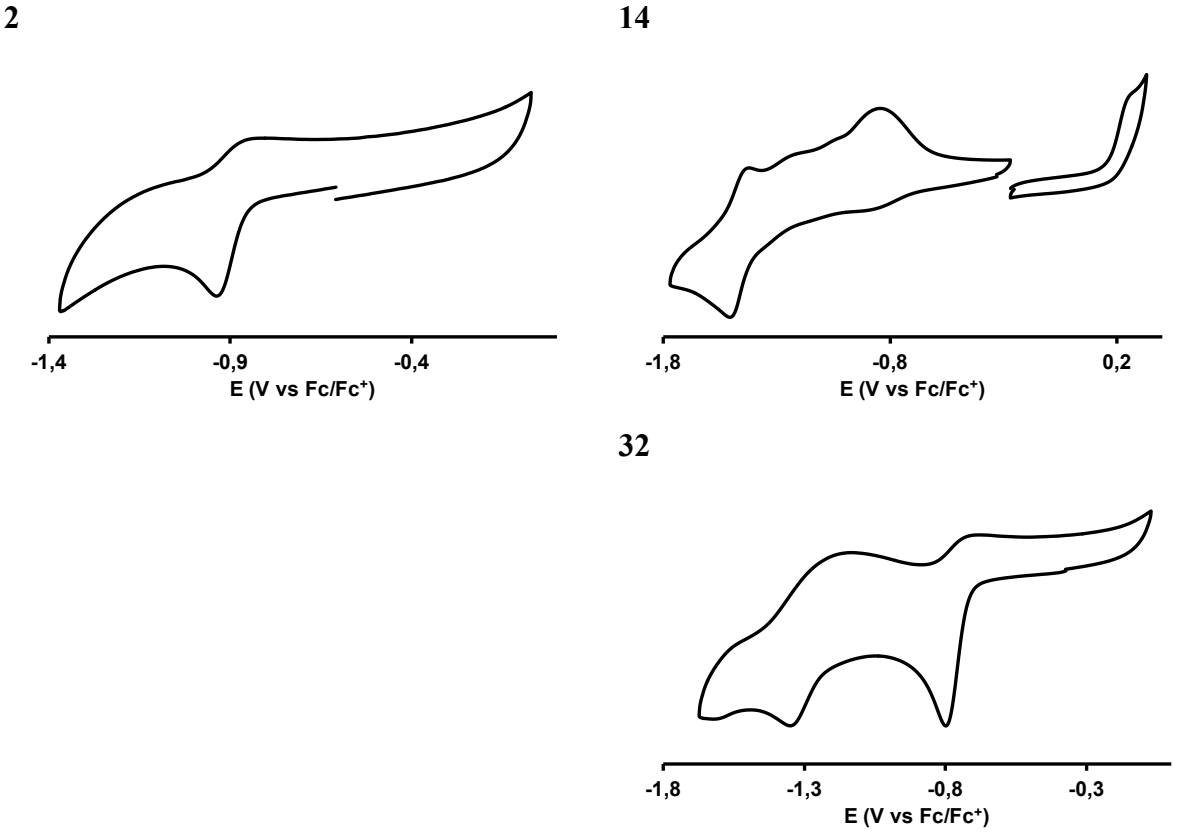

Figure S6. Cyclic voltammograms of compounds **2**, **14**, and **32** in DMF containing *n*-Bu_4NPF_6 (scan rate: 100 mV/s).

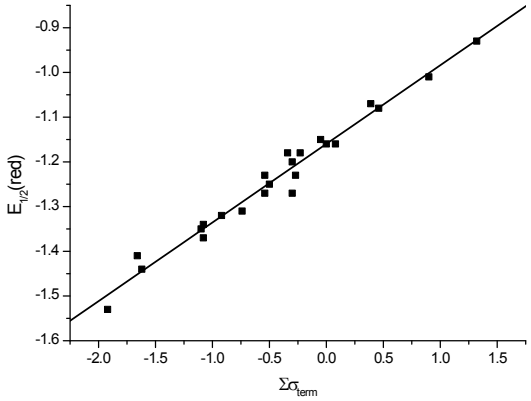

Figure S7. Plot of the correlation of reduction potential with Hammett constants

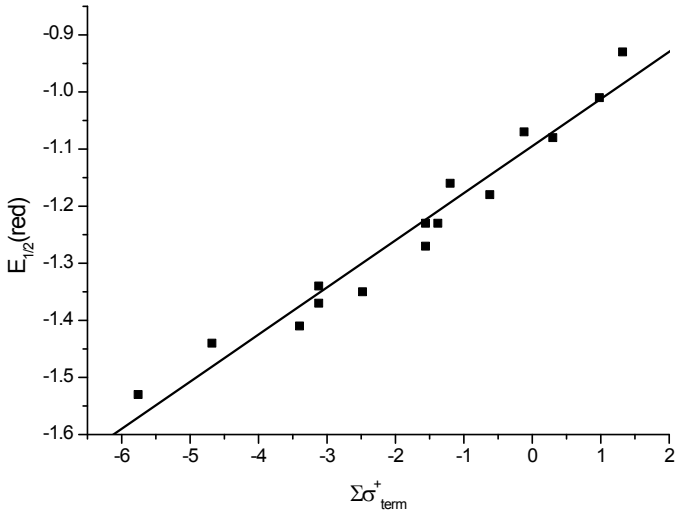

Figure S8. Reduction potential as a function of the resonance parameters σ^{+}.

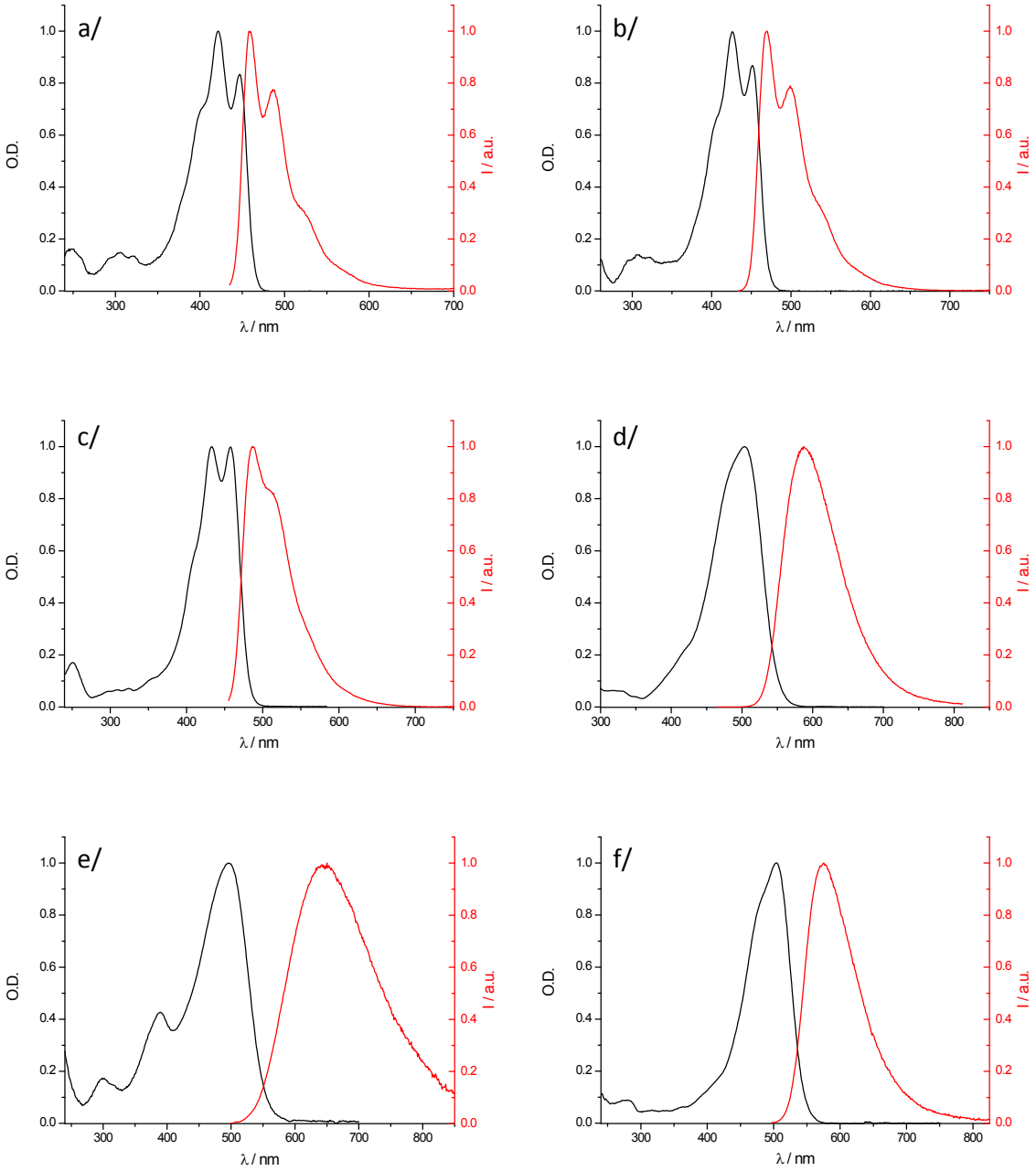
a/
b/
c/
d/
e/
f/
O.D.
I / a.u.
λ / nm

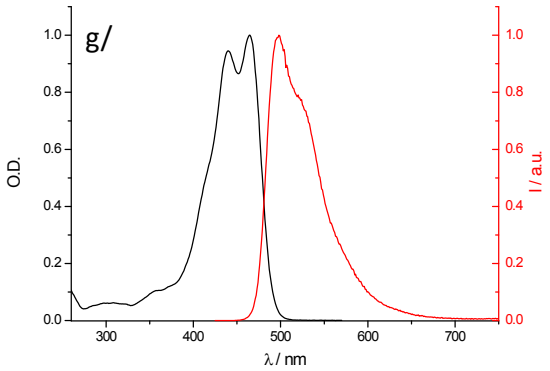
g/
O.D.
I / a.u.
λ / nm

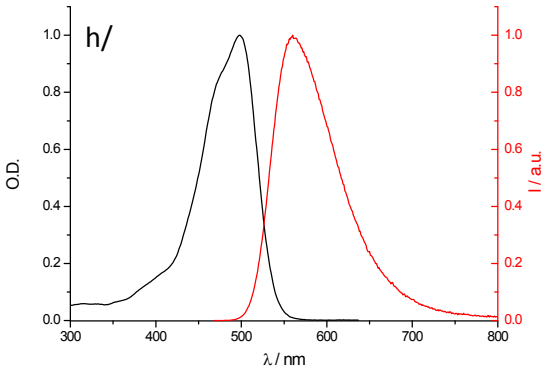
h/
O.D.
I / a.u.
λ / nm

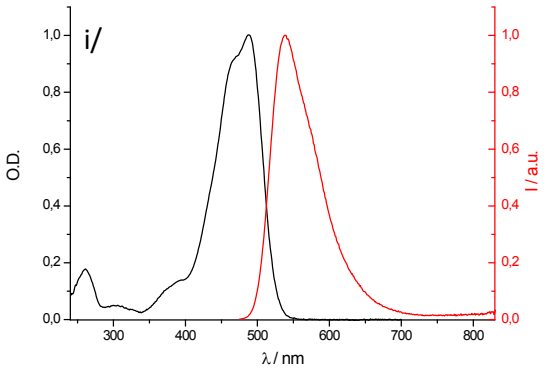
i/
O.D.
I / a.u.
λ / nm

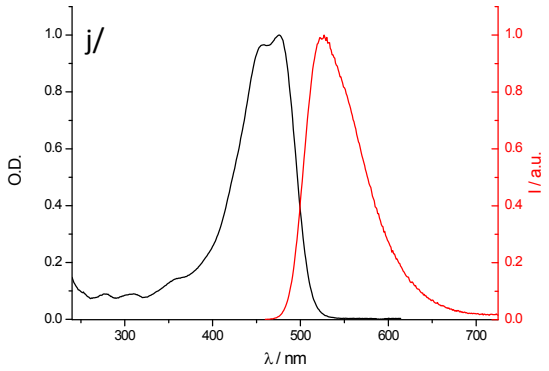
j/
O.D.
I / a.u.
λ / nm

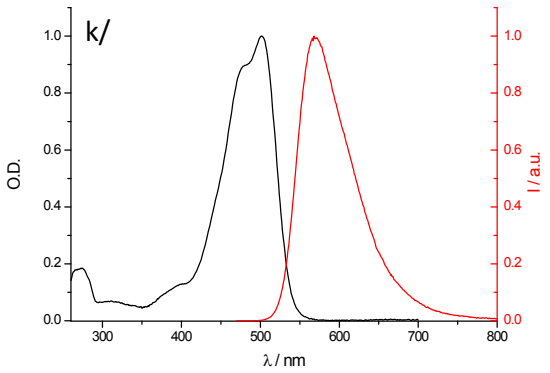
k/
O.D.
I / a.u.
λ / nm

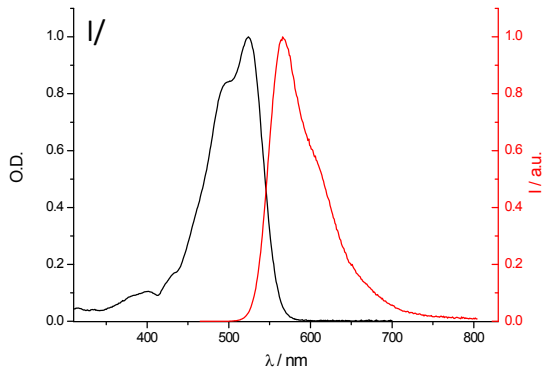
l/
O.D.
I / a.u.
λ / nm

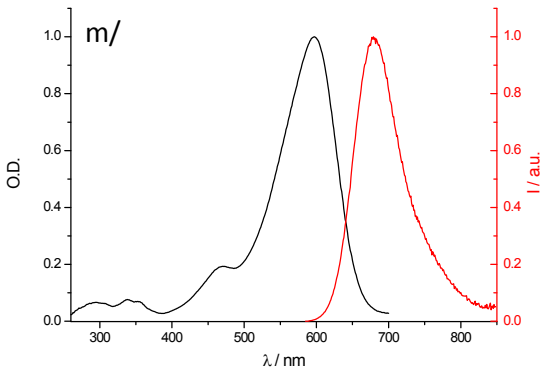
m/
O.D.
I / a.u.
λ / nm

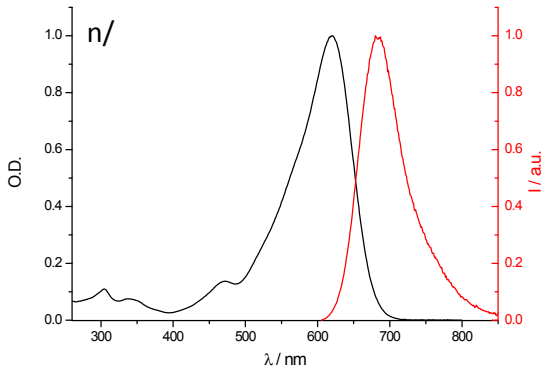
n/
O.D.
I / a.u.
λ / nm

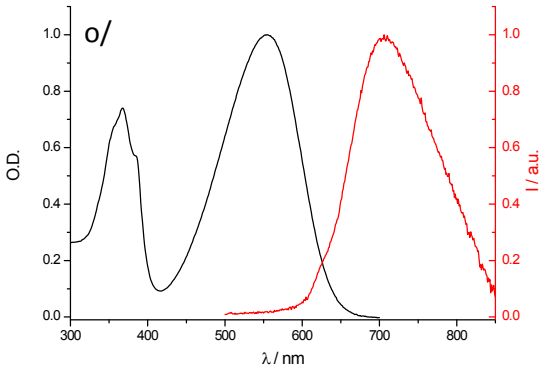
o/
O.D.
I / a.u.
λ / nm

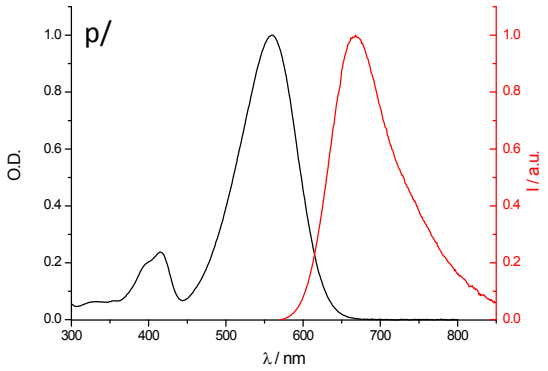
p/
O.D.
I / a.u.
λ / nm

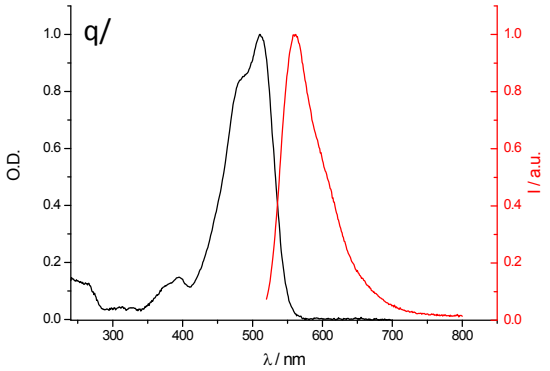
q/
O.D.
I / a.u.
λ / nm

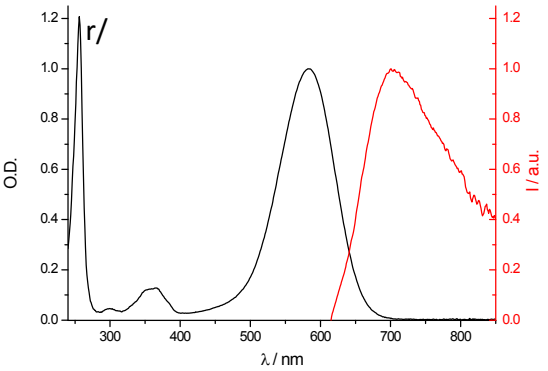
r/
O.D.
I / a.u.
λ / nm

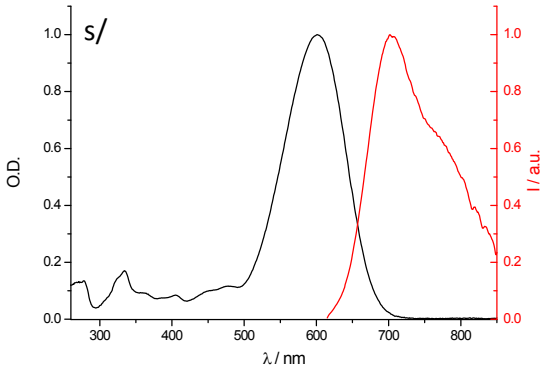
s/
O.D.
I / a.u.
λ / nm

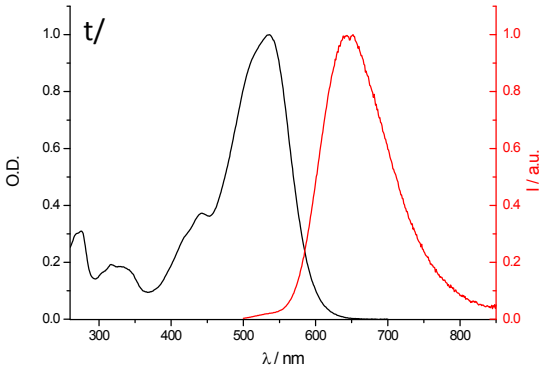
t/
O.D.
I / a.u.
λ / nm

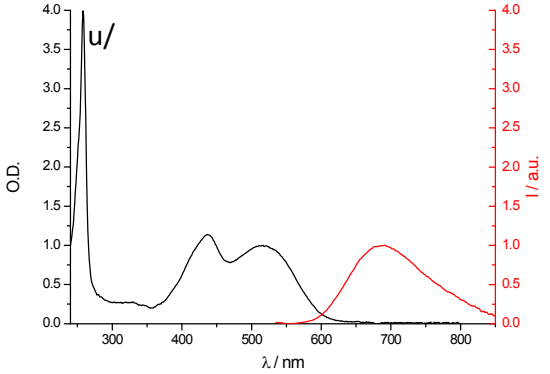
u/
O.D.
I / a.u.
λ / nm

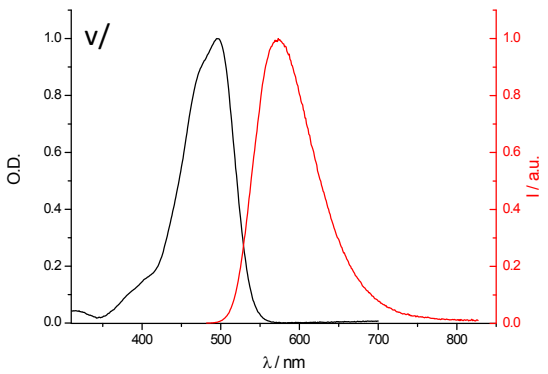
v/
O.D.
I / a.u.
λ / nm

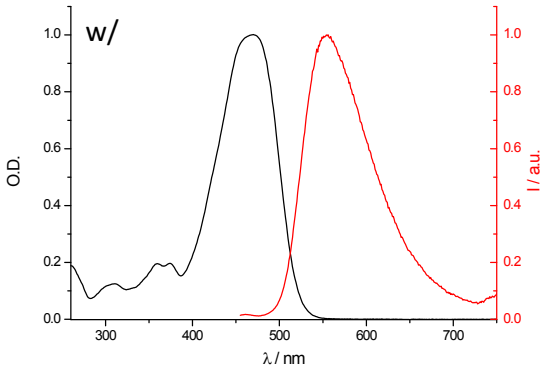
w/
O.D.
I / a.u.
λ / nm

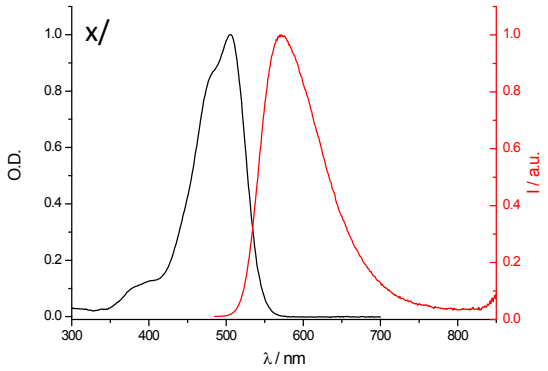
x/
O.D.
I / a.u.
λ / nm

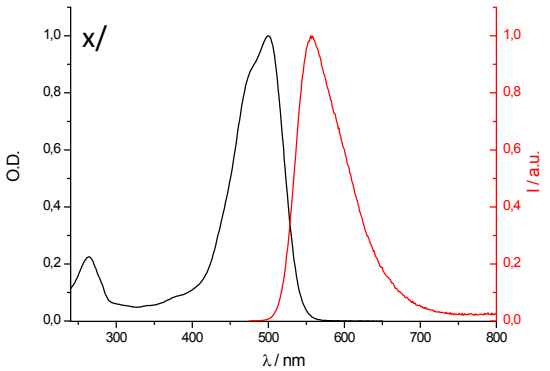
x/
O.D.
I / a.u.
λ / nm

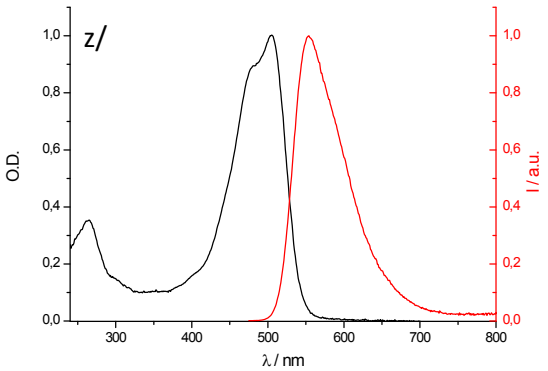
z/
O.D.
I / a.u.
λ / nm

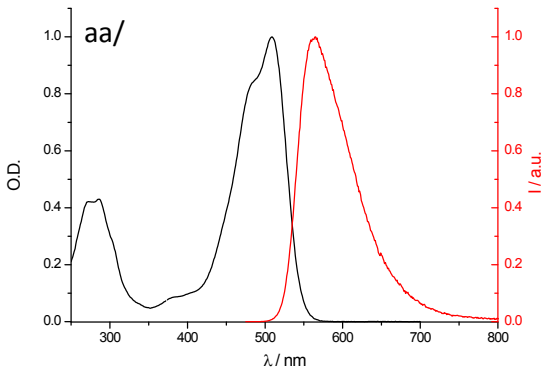
aa/
O.D.
I / a.u.
λ / nm

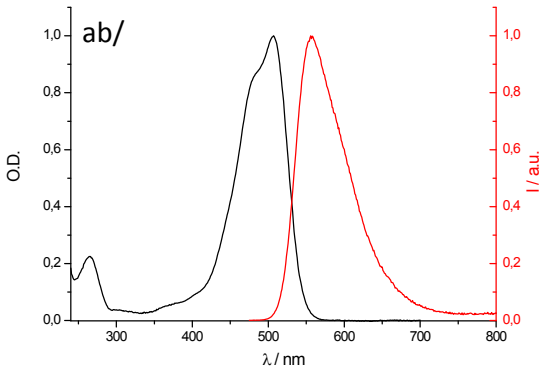
ab/
O.D.
I / a.u.
λ / nm

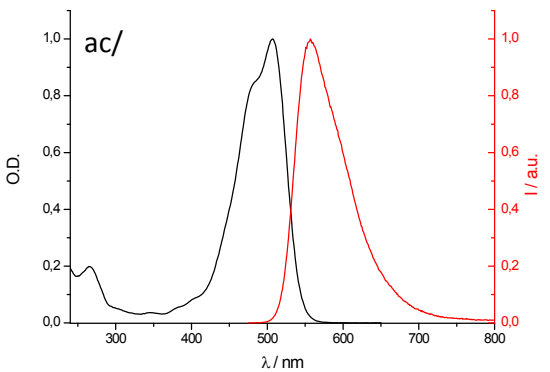
ac/
O.D.
I / a.u.
λ / nm

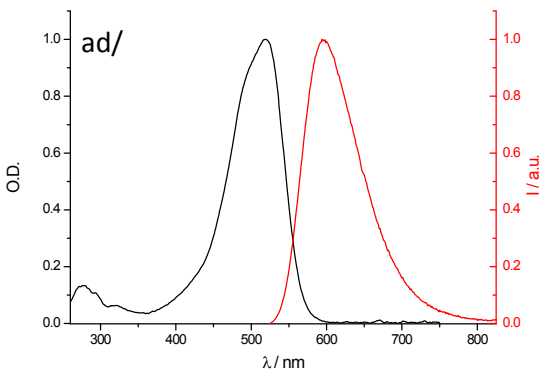
ad/
O.D.
I / a.u.
λ / nm

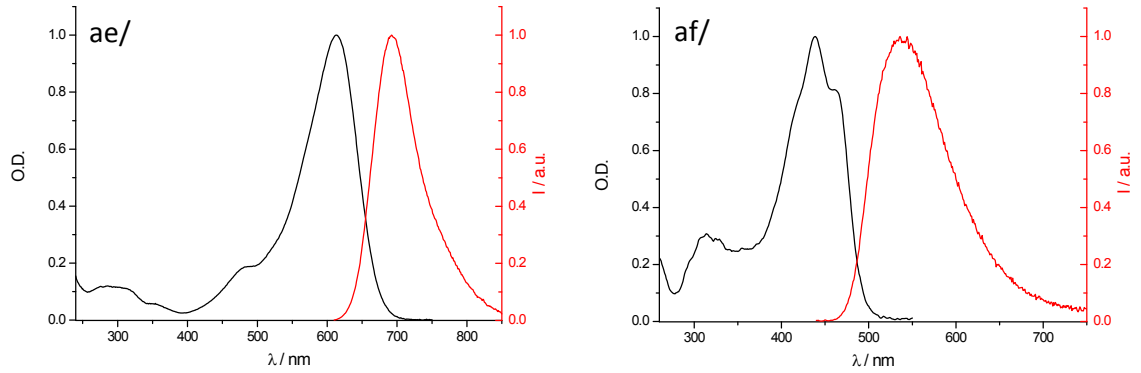

Figure S9. Electronic absorption and fluorescence emission spectra in DCM at room temperature of compounds a/ **1**; b/ **2**; c/ **3**; d/ **4**; e/ **5**; f/ **6**; g/ **7**; h/ **8**; i/ **9**; j/ **10**; k/ **11**; l/ **12**; m/ **13**; n/ **14**; o/ **15**; p/ **16**; q/ **17**; r/ **18**; s/ **19**; t/ **20**; u/ **21**; v/ **22**; w/ **23**; x/ **24**; y/ **25**; z/ **26**; aa/ **27**; ab/ **28**; ac/ **29**; ad/ **30**; ae/ **31** and af/ **32**.